

S&G 3730

Non-biennial Project UNI/532

Characterization of Undrained Behaviour of
Christchurch Soils

Prepared for EQC

Principal Investigator: Sean Rees

07

Non-biennial Project UNI/532:

Characterization of undrained behaviour of

Christchurch soils

Report prepared for the New Zealand Earthquake Commission
(EQC)

Project Leader: Misko Cubrinovski

Principal Investigator: Sean Rees (PhD Candidate)

University of Canterbury
Department of Civil Engineering

August 2007

Executive Summary

Background: Undrained behaviour and liquefaction resistance of sands with fines are not fully understood by the geotechnical engineering community. There exists an uncertainty as to the role the finer particles (such as silts) play in this behaviour. Research as part of a PhD study has been investigating this through the use of triaxial testing in the laboratory at the University of Canterbury. New triaxial apparatus was purchased and installed in June 2006, with some project and student support being provided by the Earthquake Commission (EQC). This report summarizes the activities and results from the first year of a long-term study on the characterization of undrained behaviour of Christchurch soils.

Motivation: Given the somewhat special nature of the sediments in the region of Canterbury (highly variable, loose wind-blown, alluvial deposits, with a predomination of fines), there is great interest both academically and practically as to their essential behaviour. The fact that laboratory data on these soils is quite limited and that no systematic experimental studies have been conducted to date, highlighted the need and was the motivation for this study. The principal goal of the long-term study is to establish a general framework for improved geotechnical characterization, design and performance assessment of engineering structures during strong earthquakes. This will include two major contributions in this area through the development of: (1) experimental database on deformational behaviour of Christchurch soils, and (2) generalized characterization model for undrained behaviour and liquefaction of sands with fines.

Testing procedures: A newly acquired advanced triaxial testing apparatus was used for testing of reconstituted soil specimens in the laboratory. First, a series of tests were performed on samples of clean Albany sand as verification for the new apparatus. These tests included monotonic and cyclic loading under both drained and undrained conditions. Typical liquefaction tests as well as shear modulus degradation tests ($G-\gamma$ curves) were conducted. Results indicated that correct calibration of the apparatus had been achieved, with a number of corrections to the whole test setup being made over the course of this testing stage. The calibration and verification phase was then followed by a careful development of detailed and competent testing procedures. A method was devised to enable quality test specimen preparation, with specimens being prepared using the moist tamping placement method.

Principal test series: Following the complete verification of the apparatus and establishment of appropriate testing procedures, a series of tests was performed on soil samples taken from a local Christchurch site (Fitzgerald Bridge). The soil containing about 10 % fines was used to prepare reconstituted samples in the laboratory and to test

them using both monotonic and cyclic loading under undrained conditions. The monotonic tests provided stress-strain behaviour for various relative densities of the soil ranging between $D_r = 23\%$ and 73% and allowed the steady state line for the soil to be determined. This is useful in predicting undrained soil behaviour tendencies within the state concept framework, which is the cornerstone of the adopted modelling approach in this study. The concept allows distinguishing between contractive and dilative behaviour of the sand based on its initial state and identifying states that exhibit strain softening behaviour which is particularly damaging because of the associated instability and large ground deformation. In addition to the monotonic tests, a series of cyclic tests (liquefaction tests) provided data defining the cyclic strength of the soil (liquefaction resistance curves), which correlates the number of cycles or intensity of earthquake ground motion required to induce liquefaction.

Over the past two months a similar tests series as above have been under way for the Fitzgerald soil with removed fines ($F_C = 0\%$). The comparison of the results from the two series of tests on samples with $F_C = 10\%$ and $F_C = 0\%$ will allow evaluation of the effects of fines on the undrained behaviour. The second test series is still in progress.

Key findings: The position of the steady state lines in the $e-p'$ plot for the two tested soils is clearly correlated to the amount of fines and is consistent with findings from a previous study on the subject (Cubrinovski and Ishihara, 2000). These results indicate that only very loose samples of clean Fitzgerald sand will exhibit fully contractive behaviour under monotonic undrained loading and that 10% of fines will significantly increase the number of initial $e-p'$ states showing contractive behaviour. These results are encouraging because they indicate that these soils could be explained within the generalized framework established for other sandy soils.

The cyclic tests are still in progress and their results and interpretation could not be discussed at the time of completion of this report.

Future research: The research will continue to use the Fitzgerald sand as a base material. After testing the original mix with 10% fines ($F_C = 10\%$), and removing the fines to test the host sand only ($F_C = 0\%$), in the next two series of tests the fines will be re-introduced at a greater content for further testing of soils with $F_C = 20\%$ and 30% . The data from the four series of tests will be used for investigation of the effects of fines on both monotonic and cyclic undrained behaviour including liquefaction resistance and development of a model for geotechnical characterisation of these soils. A number of Christchurch soils will then be tested to verify this model and provide basis for its application to a wide range of native sandy soils in Christchurch.

Plain English Summary

Strong earthquakes are recognized as one of the principal natural hazards for New Zealand. The intense ground shaking during such earthquakes may cause damage to wooden houses, buildings, bridges and industrial facilities, loss of function of lifelines (water and electricity supply), and will affect the society in a very profound way.

All these structures and lifelines rest on the ground or are buried into it, and therefore, it is critically important to know how the ground will behave during strong earthquakes. Typically, soils are saturated in their natural state and contain a significant amount of water. During strong shaking, the pressure in the water will increase and this will lead to “softening” of the soil. In other words, the soil will lose some of its strength and capacity to support the structures resting on it. In the extreme case, the soil may liquefy and completely lose its strength. The “quick-sand” illustrates well this state of the soil. The pore pressure build-up, eventual liquefaction and consequent deformation of soils are all embodied in the technical term “undrained behaviour” of soils.

The undrained behaviour of soils depends on their grain-size composition. Clays having very fine particles respond to earthquakes in a very different way from sands, which have particles between 0.06 mm and 2 mm and are recognized as the most susceptible soils to liquefaction. The effects of fines on the undrained behaviour of sands are quite complex and not well understood. This is a particularly relevant issue for Christchurch because this city has highly variable sandy deposits with a predomination of fines and relatively high seismic hazard.

This report presents the initial phase of an experimental study on the undrained behaviour of Christchurch soils carried out at the University of Canterbury under the support of EQC. Since soil testing is quite complex and based on rigorous procedures, the first phase of the study was used to verify the performance of a newly acquired apparatus and to establish testing procedures for the Christchurch soils. In the second phase, soil samples were collected from several sites in Christchurch and were tested in the laboratory. In these tests, the soils were loaded in a way that resembles the loads imposed on field deposits during actual earthquakes. A series of tests were conducted on two soils with different fines contents ($F_C = 0\%$ and 10%) in order to investigate the effects of fines on undrained behaviour. This report summarizes the results of the laboratory tests.

The ultimate goal of this long-term study is the development of a geotechnical model that will allow reliably predicting the behaviour of Christchurch soils during strong earthquakes. This in turn will result in an improved design and performance of engineering structures during extreme seismic events.

Abstract

The undrained behaviour and liquefaction potential/strength of sands with fines are not fully understood by the geotechnical engineering community. There exists an uncertainty as to the role the finer particles (such as silts) play in this behaviour. Research as part of a PhD has been investigating this through the use of triaxial testing in the laboratory at the University of Canterbury. New triaxial apparatus was purchased and installed in June 2006, with some project and student support being provided by the Earthquake Commission (EQC) at this time as well. A method was devised to enable quality test specimen preparation, with specimens being prepared using the moist tamping placement method. Procedures for drained and undrained loadings were developed to gain the best possible data from the new triaxial apparatus. A clean Albany Sand was the first soil to be used for testing in this research. These tests were performed as verification for the new apparatus, with drained monotonic, undrained monotonic and undrained cyclic tests being completed. Results indicated that correct calibration of the apparatus had been reached, with a number of corrections to the whole test setup being made over the course of this test stage. Following this, a silty sand mixture was created from soil samples taken from a local Christchurch site investigation. This Fitzgerald Soil Mix was tested (first stage) using both undrained monotonic and cyclic loadings. The monotonic tests allowed the steady state line for the soil to be determined. This is useful in predicting undrained soil behaviour tendencies. The cyclic tests provided data to create liquefaction curves, which indicate the requirements for cyclic liquefaction based on the applied Cyclic Stress Ratio (CSR), number of cycles, and specimen density. The research will continue to use this soil as a base material – the fines will be removed to enable testing as a clean sand (second stage), before fines are re-introduced at a greater content for further testing (third stage). This data will be used in the creation of a model enabling characterisation of silty sands and their undrained behaviour. A number of Christchurch soils will then be triaxially tested to verify this model, and add to the information base on Christchurch soil liquefaction potential/strength.

TABLE OF CONTENTS

ABSTRACT.....	1
1. INTRODUCTION.....	3
2. BACKGROUND.....	5
2.1 TEST METHODS	6
2.2 UNDRAINED BEHAVIOUR OF SANDS WITH FINES	9
2.3 CHRISTCHURCH SOILS.....	14
3. SETUP OF APPARATUS.....	16
3.1 PRESSURE CONTROLLERS	17
3.2 MOTORISED TRIAXIAL CELL.....	18
3.3 SERIAL DATA ACQUISITION PAD	19
3.4 PC SETUP	20
3.5 WATER DE-AERATOR.....	20
4. SPECIMEN PREPARATION AND TESTING PROCEDURE	22
4.1 SPECIMEN PREPARATION	22
4.1.1 Mould preparation.....	22
4.1.2 Soil Reconstitution	25
4.2 TESTING PREPARATION	28
4.3 SPECIMEN LOADING	33
4.3.1 Monotonic Loading.....	33
4.3.2 Cyclic Loading.....	34
4.4 POST-TEST PROCEDURE	34
5. ALBANY SAND TRIAXIAL TESTS (APPARATUS VERIFICATION)	37
5.1 DRAINED MONOTONIC TRIAXIAL TESTING.....	37
5.2 UNDRAINED MONOTONIC TRIAXIAL TESTING	41
5.3 UNDRAINED CYCLIC TRIAXIAL TESTING	46
5.4 ALBANY SAND TRIAXIAL TESTING SUMMARY	50
6. TRIAXIAL TESTS ON FOUNDATION SOILS OF FITZGERALD BRIDGE ..	52
6.1 FITZGERALD BRIDGE SOIL MIX	52
6.2 SOIL PREPARATION.....	54
6.3 SPECIMEN PREPARATION	55
6.4 UNDRAINED MONOTONIC TRIAXIAL TESTS	55
6.5 UNDRAINED CYCLIC TRIAXIAL TESTS	61
6.6 FITZGERALD SOIL MIX TRIAXIAL TESTING SUMMARY	67
7. FUTURE RESEARCH.....	68
7.1 CLEAN SAND TESTING	68
7.2 SILTY SAND TESTING	69
7.3 SILTY SAND CHARACTERISATION MODEL	69
7.4 NATURAL CHRISTCHURCH SOIL TESTING	70
8. REFERENCES.....	72

1. Introduction

The major earthquakes of Alaska and Niigata in 1964 highlighted the need for the geotechnical engineering discipline to consider designing for liquefaction. The effects of these earthquakes included extensive liquefaction and settlements of 1m to buildings, ground surface cracking and sand boils, landslides and movement of abutments (Seed and Idriss 1982). These events led to research furthering the understanding of liquefaction, and the creation of investigation and design methods to mitigate the effects of this phenomenon.

Early works in this field of geotechnical engineering coined the term liquefaction, referring to the response of saturated loose sand deposits to strains which resulted in flow slides (Casagrande 1979). This was used until 1966, when the term was split into two separate types of behaviour: flow liquefaction and cyclic mobility. Flow liquefaction describes the initially observed behaviour of soil deposits moving through large deformations due to a loss in strength, while cyclic mobility describes a soil deposit retaining strength but deforming due to the constant application of cyclic loads.

Past evaluation of liquefaction potential and resistance has used two methods: field (in-situ) testing and laboratory testing. Field testing has generally been associated with use of the Standard Penetration Test (SPT) and the Cone Penetration Test (CPT); laboratory testing has often used triaxial testing apparatus. These methods, combined with theoretical reasoning, have provided good insight to the liquefied behaviour of clean sands. However, the behaviour of sands containing finer particles (such as silts and clays) has not been as clearly understood. Disagreement exists in literature as to what effect fines play in the behaviour of soils such as silty sands between each type of liquefaction. The flow potential under monotonic loading of such soils is observed to increase with increasing fines content in some studies (Cubrinovski and Ishihara 2000), whilst other research on cyclic behaviour shows increasing resistance to liquefaction with increasing fines content (Youd and Idriss 2001).

Such differences in behaviour between the two types of liquefaction need to be explained. This research (as part of a PhD) has been investigating the undrained behaviour of soils with fines under both monotonic and cyclic loading, using conventional triaxial testing apparatus. This enables direct comparison between the two loading methods. Future work as part of the research will compare a number of other variables such as relative density, the state parameter and void ratio range. Analysis of the data to be obtained will help to identify the best parameter for describing the initial state of soils containing fines with respect to their liquefaction potential and resistance. Improvements to current design methods, or new methods, may also arise from this testing and analysis phase.

Christchurch soils are being used for the majority of the testing. Located in the South Island of New Zealand, the city of Christchurch lies on highly variable soils. It sits on the youngest postglacial fan surface of the Waimakariri River, and has soils containing gravel, sand, silt, clay and peat (Brown et al. 1992). Using these soils in the triaxial testing will provide information on these soils not previously tested for in the laboratory. This will also further assess the liquefaction potential and resistance for specific locations in the city.

2. Background

Flow liquefaction and cyclic mobility are the two components of the phenomenon referred to as liquefaction. Flow liquefaction occurs when the shear strength of a soil deposit is reduced through a build-up in pore water pressure. When the strength drops below the magnitude of the static shear stresses being applied to the deposit (Kramer 1996), such as from the weight of the soil, a catastrophic flow failure may occur. In this case the static stresses drive the failure. This phenomenon is associated with strain softening and large-scale deformations, typically being slope failures (for example the failure of the Lower San Fernando Dam) (Baziar and Dobry 1995). This concept is shown in Figure 1 in terms of effective stress paths and stress-strain curves.

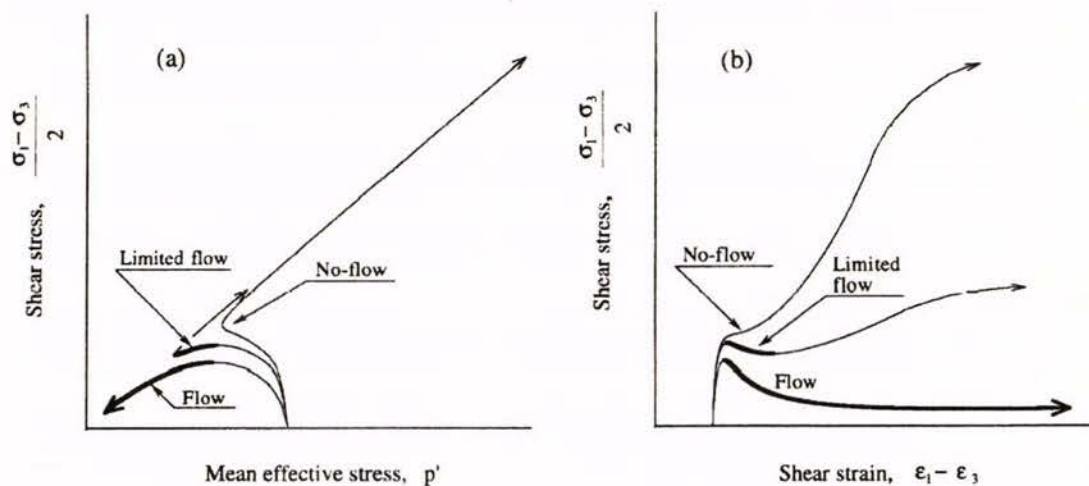


Figure 1 - Behaviour of typical soil undergoing flow liquefaction and no-flow (Cubrinovski and Ishihara 2000).

Cyclic mobility occurs when incremental deformations develop due to pore pressure build-up and softening of the soil caused by cyclic loading (usually an earthquake). Here both the static and cyclic stresses drive the deformations.

Each of these types of behaviour can cause high levels of damage both to infrastructure and land formations. Flow liquefaction is generally the most destructive, due to the large deformations involved. Case histories include such slides as the Sheffield Dam (1925),

Fort Peck Dam (1938), Juvenile Hall landslide (1971), and the Mochi-Koshi Tailings Dam (1979), as well as many cases of embankment and building foundation failures (Seed 1987). Cyclic mobility is generally less destructive due to smaller deformations, but still can cause significant damage such as building settlement, failure of pile foundations, lifeline breakages (water pipes etc), quay wall movements and bridge abutment displacements.

2.1 Test Methods

Methods for developing an understanding of liquefaction behaviour require methods for testing soils. These can be divided into two groups: field testing (in-situ) and laboratory testing. The most widely used field test has been the SPT. This involves driving a sampling probe 30cm into the soil layer and recording the number of blows required for the penetration. This number is the N-value, standardised to $(N_1)_{60}$, and it is this property which has been used to correlate liquefaction potential with in-situ soil conditions. Seed and Idriss developed their simplified method in 1971, which although revised, is still in practical use today. This method created design curves to assess whether liquefaction will occur, using site N-values and an estimation of shear stresses generated in an earthquake. An example of such a curve is shown in Figure 2. Note how the resistance to liquefaction tends to increase with increasing fines content. The dividing line between liquefaction and no liquefaction occurs at lower $(N_1)_{60}$ blow counts for 35% fines than for 0% fines.

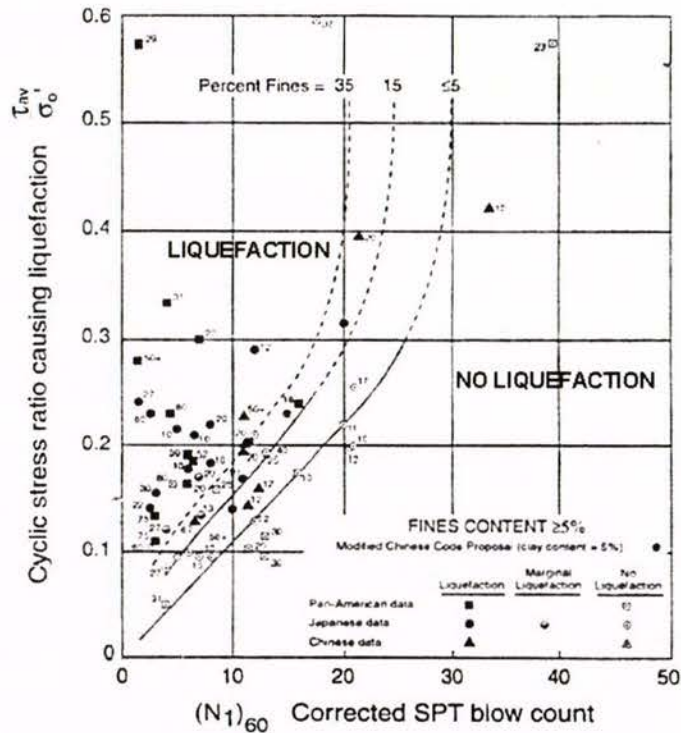


Figure 2 - Design curves separating liquefaction and no liquefaction using initial in-situ conditions (Seed et al. 1985).

The predominant method for laboratory testing has been the use of triaxial shear apparatus. This involves confining a soil sample (confining stress, p) and applying an axial load (creating a deviator stress, q) to cause shearing within the soil. Properties such as deviator stress, axial strain and pore water pressure (or volume change of the sample) are measured to enable characterisation of the stress-strain behaviour under shearing. Both flow potential and liquefaction strength testing require undrained shearing conditions, resulting in no sample volume change. Generalised framework such as the steady-state concept can be used to characterise the undrained monotonic loading behaviour relative to the initial soil state (initial density and confining stress state). Once the steady-state line is known, it enables us to divide between regions of flow liquefaction and no-flow in the e - p' plane, as illustrated in Figure 3.

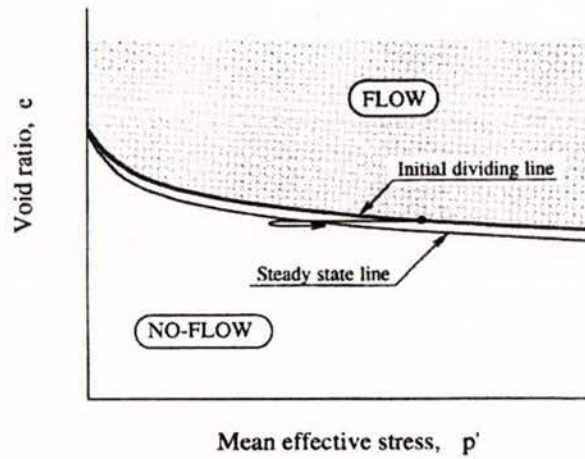


Figure 3 – Steady-state line separating flow and no-flow initial conditions (Cubrinovski and Ishihara 2000).

Each of these testing methods have advantages and shortcomings. Field testing with the SPT does not give constant readings for the entire depth of penetration, but can provide soil samples. A CPT can be used to substitute/supplement SPT data, as the CPT gives a continuous resistance reading, helping to identify thin layers of soil. The major shortcomings of these tests is they do not load the soil like an earthquake would, so we have to correlate penetration resistance with liquefaction observations from previous earthquakes. The advantage of these tests is they do not require movement of the soil, and test in-situ.

The triaxial test has a number of issues. This test firstly requires representative soil samples to be taken from the field and transported to the laboratory, where they must then be prepared in the triaxial apparatus. This process is generally very disruptive for the soil sample, and greatly alters the initial state of the soil before testing, compared to the in-situ state. In particular, the disruption affects key parameters such as relative density and soil fabric, both of which influence the undrained behaviour and liquefaction resistance of a soil. Ground freezing is generally regarded as the best method for obtaining high quality undisturbed samples, but is also expensive. This means disturbed or reconstituted samples are most often tested. A number of issues also arise during the preparation and testing phase, including sample preparation method, membrane penetration, volume

changes during saturation and consolidation, and end cap friction. These issues can be accounted for with correction factors. Triaxial testing also requires conversion of the stress ratio, as this is not representative of simple shearing conditions. This is done using the C_r factor (Seed 1979). Overall the triaxial apparatus can be used effectively to provide accurate information on the deformational behaviour and strength of soils; the main issue is reconstituting or obtaining quality samples.

The reconstitution of soil to create samples ready for triaxial testing is particularly important. This is due to previous research (Ladd 1974), (Høeg et al. 2000) showing that preparation method directly affects the fabric of the soil, which in turn directly affects the behaviour when sheared. Methods such as slurry-based preparation (Carraro and Prezzi 2006) have been shown to give stress-strain response in testing that resembles those of natural deposits formed under water. Water pluviation is also a preparation method considered to give a reasonably similar fabric to that of hydraulically deposited fills. Other methods such as moist tamping have been shown to underestimate the strength of the soil being tested, compared with undisturbed samples (Høeg et al. 2000). The choice of preparation method (if reconstituting) must be made with type and age of deposit in mind to achieve the most similar soil fabric possible.

2.2 Undrained Behaviour of Sands with Fines

The undrained behaviour of clean sands (sands with less than 5% particles by mass passing a 75 μ m sieve) is generally understood. Looser sands, with higher void ratios and lower relative densities, are generally more susceptible to flow liquefaction or cyclic mobility as they are more susceptible to compression. This susceptibility to compression causes excess pore water generation in undrained conditions, which lowers the effective stress for the soil deposit. This creates a soil which has a lower capacity to resist deformations, due to either static or cyclic loadings. The confining pressure also has a major effect on soil behaviour, as larger confining pressures tend to promote contraction of the soil. This gives a general model for clean sand behaviour when sheared: at a given

relative density a sand sample is more dilative at lower confining pressures, with increasing contractive behaviour as confining pressure is increased. This behaviour is shown in the effective stress paths in Figure 4.

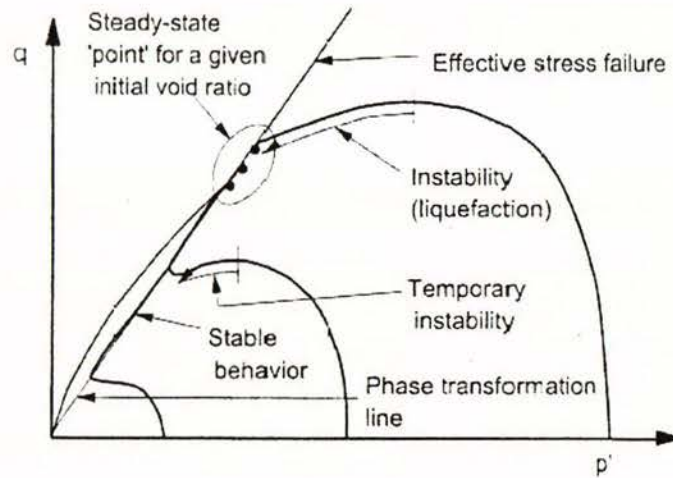


Figure 4 – Stress paths showing general behaviour for a typical clean sand (Yamamuro and Covert 2001).

The behaviour can also be considered in terms of sand particle deformation during shearing: for example, at lower pressures the particles tend to roll over each other and rearrange. These sort of general observations tend to change however when the sand includes finer particles.

Sands with only a small amount of fines (around 5%) have been shown to exhibit “reverse” behaviour when sheared in undrained conditions (Yamamuro and Covert 2001). This involves compressive behaviour at low confining pressures which can lead to full liquefaction of samples. A general example of this is displayed in Figure 5, showing static liquefaction at low p' .

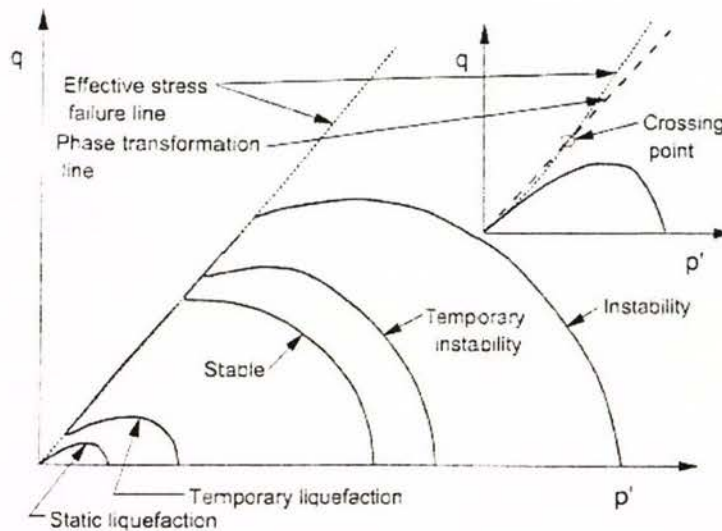


Figure 5 – Stress paths showing general behaviour for a typical silty sand (with less than 30% fines) (Yamamuro and Covert 2001).

This is the opposite behaviour of clean sands, where low pressures usually allow dilative behaviour. It has been suggested that this behaviour occurs due to the range of particle sizes and their interaction. The theoretical model involves considering a gap-graded soil with sand particles and silt particles. In such a soil, the fine silt particles can either sit between the sand grains (in the void space) or between the sand grain contacts (holding the sand grains apart). This is shown in Figure 6. The latter case leads to a very loose, compressible soil, as the application of stress causes the fine silt particles into the void spaces. This gives rise to compressive behaviour during shearing at low confining pressures. It has also been noted in previous studies (Baziar and Dobry 1995) that a large number of flow liquefaction failures have occurred in soil deposits containing a reasonable amount of fines (15%-30%), including the Sheffield Dam, Fort Peck Dam and Lower San Fernando Dam failures. This shows the issues involved with silty sand liquefaction are very relevant to field cases.

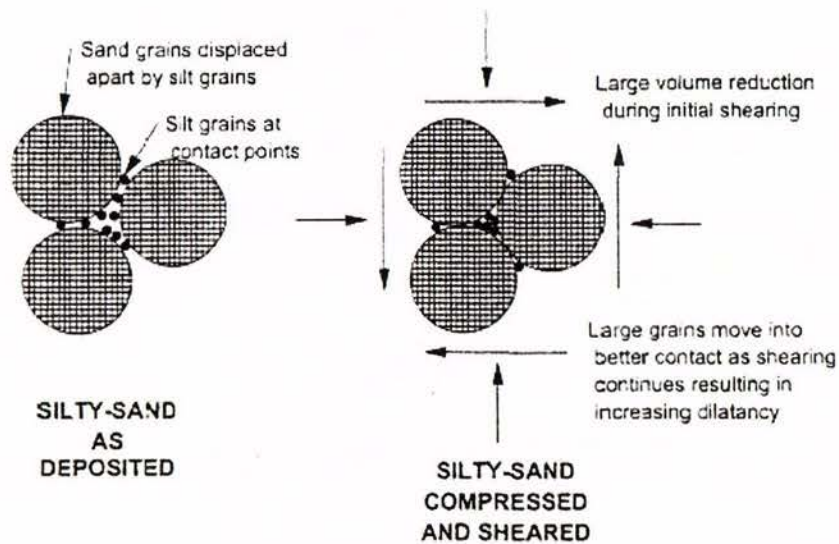


Figure 6 – Theoretical behaviour of gap-graded silty sand (Yamamuro and Covert 2001).

The nature of sands containing fines is therefore much more complex than for clean sands, due to the variability in packing and effects of fines. This means that a parameter such as relative density (D_r) which has been used to characterise the liquefaction potential for clean sands cannot as easily describe the potential behaviour for a silty sand, even with low silt contents.

One parameter possibly useful for characterising silty sands is the maximum and minimum void ratio difference, ($e_{max}-e_{min}$). This parameter considers the maximum and minimum void ratios for a given soil, and has been found to increase with increasing fines content (Cubrinovski and Ishihara 2002). It has also been shown that a higher ($e_{max}-e_{min}$) value gives a soil more potential to exhibit flow liquefaction. This is due to the initial dividing line between flow and no-flow moving towards higher D_r values, meaning that higher D_r values can exhibit flow liquefaction, and is displayed in Figure 7. It implies that sands with higher silt contents have more potential for flow liquefaction. This parameter ($e_{max}-e_{min}$) has not been applied to cyclic mobility testing, which considers cycles at a specific cyclic stress ratio to reach a certain amount of strain (usually 5% double amplitude). It would be of great benefit to test silty sands in shear (using both monotonic and cyclic loadings) and compare the usefulness of a number of parameters

including relative density D_r , state parameter ψ , state index I_s and void ratio difference ($e_{max}-e_{min}$).

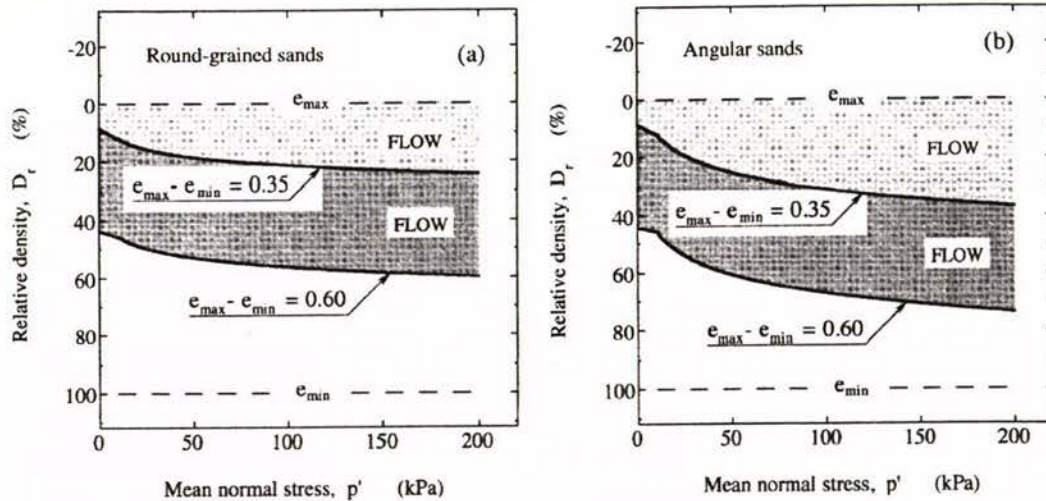


Figure 7 – Steady-state lines for certain ($e_{max}-e_{min}$) values, dividing initial conditions for flow liquefaction and no-flow (Cubrinovski and Ishihara 2000).

The behaviour of silty sands as shown in Figure 5 and Figure 7 display a difference in the effects of fines to those given by results in Figure 2, where liquefaction resistance increases with increasing fines content. The works by Seed (and others) comparing the CSR with $(N_1)_{60}$ suggest that more fines in a sand will reduce liquefaction potential, due to silty sands being able to resist cyclic mobility with lower N-values than for clean sands. This is seemingly in direct contrast to the research by Cubrinovski, Yamamuro and others that show more fines increase flow liquefaction potential.

On closer inspection however, there are numerous differences between the parameters involved in the respective research. The simplified method of Seed and Idriss uses SPT $(N_1)_{60}$ to compare against cyclic stresses, but the curves shown in these plots do not consider the effect of fines content on SPT N-value. This method also generally assumes liquefaction occurring at 5% double axial strain, whereas the steady-state lines shown in Figure 7 are derived from data at approximately 25% axial strain. It is therefore likely that differences between the seemingly conflicting research, such as those described above, are only due to differences in evaluation and testing methods, as well as the

parameters used. A testing regime investigating the effects of fines in sands, combining cyclic and monotonic loading, has the potential to properly explain these differences.

2.3 Christchurch soils

Christchurch overlies a variety of soil types, due to a number of different geological processes. The rock basement under the Canterbury Plains consists of Torlesse Supergroup rocks, much like those of the Southern Alps (Brown et al. 1992). Above these sit a gravel layer approximately 500m thick, deposited by eastward-flowing rivers in a series of complex coalescing fans. However, most of the build-on land in Christchurch was formed within the last 10000 years, in a period of rising sea-level. This extends approximately 8km inland of the coastline, and provided much of the sand found in Christchurch soils. The Port Hills are another geological feature, formed from the Lyttelton Volcano overlain by Banks Peninsula loess, a wind-blown silt derived from the Quaternary glaciations of the Southern Alps.

The two main soils under the level-ground area of Christchurch are known as the Christchurch Formation and Riccarton gravel. Christchurch Formation soils are a mixture of beach, estuarine, lagoonal, dune and coastal swamp deposits (Brown et al. 1992). This leads to a large variety of soil types and particle sizes: gravel, sand, silt, clay, shell and peat can all be found in this soil formation. This layer can vary in thickness from only a few metres down to 40m. The finer particles in this formation (mostly silts) generally have low plasticity. Riccarton gravel directly underlies the finer sediments of the Christchurch Formation, and is a well-graded gravel with a blue-grey colour due to iron reduction (Brown et al. 1992). These two soil layers represent the soil usually encountered during construction in the level-ground region of Christchurch. Other soils, such as New Brighton sand and Banks Peninsula loess are encountered on the coastline and Port Hills respectively. There is also the Springston Formation to the west of the Christchurch Formation: a postglacial fluvial channel deposit comprising well-sorted gravel, sand and silt. The variety of these different particle sizes, as listed above, shows

how variable foundation conditions can be around the Christchurch area, particularly with regard to seismic behaviour and liquefaction.

The location of the water table is of direct importance when assessing liquefaction potential for a soil. Christchurch has a relatively high water table due to the deep layers of gravel underlying the Canterbury Plains. Groundwater flows seaward from the Southern Alps within gravel aquifers, and is pushed upwards towards the surface near the coast (and Christchurch) due to high pressures (Brown et al. 1992). The groundwater also receives recharge from seaward-flowing rivers, such as the Waimakariri River. The height of the water table means that near-surface soils are generally saturated, a condition that must be satisfied if liquefaction is to occur.

The Christchurch City Council commissioned a study on the liquefaction potential of Christchurch soils, producing (amongst other information) soil liquefaction hazard and damage maps for the city in 2004 (Beca Carter Hollings & Ferner Ltd 2004). This study relied on SPT and CPT data gathered from a variety of sources. The hazard maps consider the potential hazard for liquefaction using high, moderate, low and no hazard classifications. They also contain areas with insufficient soil information to be properly classified. The liquefaction damage maps show the potential damage to an area in terms of subsidence (and lateral spreading). They also contain areas where insufficient soil information prevents a proper damage prediction.

While providing very limited basis for liquefaction evaluation, these investigations have not used any testing of Christchurch soils. Triaxial loading of these local soils will help to better estimate the potential for liquefaction and the likely damage to soil deposits should a large-magnitude earthquake strike Christchurch in the coming years. It will also enable better design for future engineering projects.

3. Setup of Apparatus

The first major task of the research was to set up new triaxial testing apparatus in the Geomechanics Laboratory at the University of Canterbury. The apparatus was purchased from GDS Instruments Limited, located in England, and arrived at the university during June 2006. The apparatus includes two pressure controllers, a serial data acquisition pad, and a motorised triaxial cell. GDSLab software was also included in the package, allowing apparatus interface with a PC to enable test control and data collection.

Initial setup of this testing apparatus was completed within two weeks of the gear arriving. This included connecting the hardware as specified in the manual, installing the GDSLab software, interfacing with the PC, and various other smaller tasks required for triaxial testing. This enabled initial triaxial tests to get underway, in order to verify the performance of the apparatus. These tests showed up a number of problems with the setup configuration, namely calibration issues for all the major apparatus parts, including the software. For example, the axial load gave readings well below what were expected during triaxial testing. Through contact with GDS Instruments via email, it was determined that values on the RFM box (a Remote Feedback Module connected to the submersible load cell) needed to be input into the motorised cell control box. These kinds of instructions were not explicitly stated in the included GDS Instruments manual, and it therefore took some time to firstly identify the issue through testing, and fix through contact with GDS Instruments. Another major problem was the interfacing between the hardware and the PC – the IEEE card connecting the two would stop working seemingly without reason. This was eventually stabilised by September 2006, although the actual cause of the issue was never fully determined.

The issues with the testing apparatus were solved by the beginning of February 2007, with the system now stable (as of June 2007). A number of test modules (programs within the GDSLab software used for different stages of a triaxial test) were also purchased in full from GDS Instruments in April 2007. This essentially means that testing

can now continue indefinitely with the current apparatus in the Geomechanics Laboratory.

3.1 Pressure Controllers

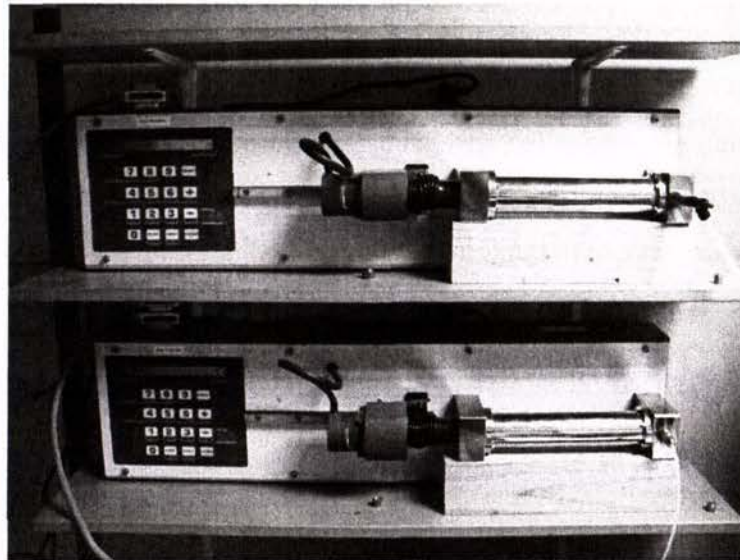


Figure 8 – Cell pressure controller (top) and back pressure controller (bottom).

The two pressure controllers are shown in Figure 8. They are both GDS Advanced Digital Controllers, and link up with the IEEE interface in the PC. These controllers are filled with de-aired water and then attached to the motorised cell. The connection points to the cell depend on the type of pressure being applied.

The cell pressure controller is attached at the bottom-left of the cell, which feeds directly into the cell chamber. With the tap open, the cell pressure controller is in direct contact with the water in the cell chamber. This water can then be pressurised by targeting a pressure on the controller, which tries to push water into the cell (through use of a piston) for increasing pressure, and remove water for decreasing pressure. The purpose for pressurising the cell water (when a soil specimen is placed inside the cell) is to simulate the effect of soil depth in the field. A soil pocket below ground surface experiences a confining pressure due to the soil sitting above it, so the cell pressure is targeted to simulate the desired depth for test purposes.

The back pressure controller is attached at the front-right of the motorised cell. This feeds into an internal cell connection, which is then attached to the base pedestal of the soil specimen. This means that the back pressure controller is used to control specimen pressure internally (as opposed to the cell pressure which acts externally on the specimen). The back pressure controller is initially used when preparing a triaxial test to percolate water through the specimen, allowing specimen saturation. After this it is used to control the pressure within the specimen. The purpose of this internal pressure is to simulate the pore pressure felt by a soil pocket in the field which is below the water table. These pressures are very important, as the build up of pore pressure during loading (an earthquake, for example) is the cause of soil liquefaction.

3.2 Motorised Triaxial Cell

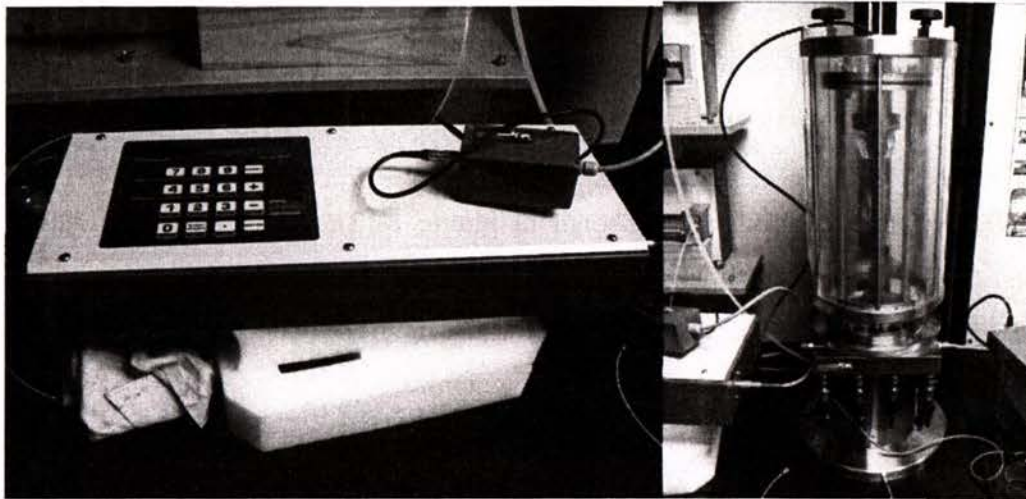


Figure 9 – Motorised cell control box (left) and motorised triaxial cell (right).

The motorised triaxial cell is shown in Figure 9, along with the motorised cell control and RFM box. The motorised cell applies an axial load by using a direct screw drive to actuate the base pedestal of the specimen, controlled by the motorised cell control box. This means that the axial load and strain are applied directly to the specimen being tested. The load is measured at the top of the cell chamber, through a submersible load cell. This is connected to the RFM (Remote Feedback Module) box, which is attached to the

motorised cell control. This system creates a loop whereby a load can be targeted on the control box, adjustments made to the axial strain, the new load determined and compared with the desired load, and the loop started again. The motorised cell control box is also interfaced with the IEEE in the PC, allowing for constant data collection. This system is used during a triaxial test for loading/straining of a specimen, and can be set to perform this in a number of different ways using the GDSLab software, such as sinusoidal stress loading or constant strain increase.

3.3 Serial Data Acquisition Pad

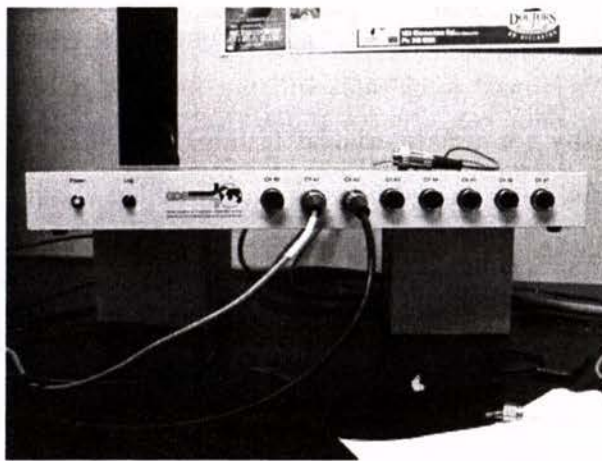


Figure 10 – Eight (8) channel serial data acquisition pad.

The serial data acquisition pad is shown in Figure 10 above. This has 8 channels available for data collection and interfaces with the PC through a Comm-port. The GDSLab software is setup to recorded data from this pad, and is currently used to log pore pressure and axial displacement. The pore pressure transducer is located in the motorised cell, and is used to monitor pore pressure from the top end of a specimen. The axial displacement also connects into the motorised cell, and monitors axial displacement of the screw drive from the base. A thermometer has been made to connect to the serial pad to monitor laboratory temperature, but this is yet to be interfaced with the GDSLab software.

3.4 PC Setup



Figure 11 – PC setup used to interface with (and record data from) the triaxial hardware.

The PC shown in Figure 11 is the setup used in conjunction with the GDS Instruments triaxial test apparatus. It was purchased with the funding grant from the Earthquake Commission specifically for use in triaxial testing. The GDSLab software, software dongle, IEEE card, and necessary drivers are all installed on this machine. It is also connected to the university network, enabling easy retrieval of test data.

3.5 Water De-Aerator

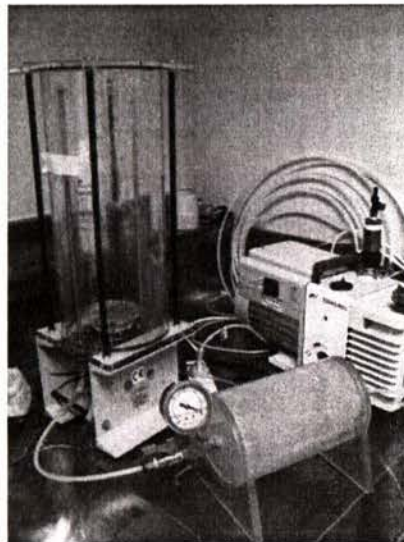


Figure 12 – The de-aerator (left), water trap (middle) and vacuum pump (right).

The setup used for de-airing water in the laboratory is shown in Figure 12. This consists of a Nold DeAerator (purchased from Geokon at the same time as the triaxial apparatus), a water trap and a vacuum pump. The de-aerator is filled directly from the tap, leaving the top 150mm free to allow air to be pumped out. Once filled, the chamber is closed off and attached to the water trap, which connects to the vacuum pump. When running, a fan at the base of the de-aerator agitates the water whilst the pump creates a vacuum that sucks air out of the de-aerator through tubes that are open to the top of the cell. This process lets air in the water rise to the water surface, and be pumped out of the cell altogether. After around 5 – 10 minutes the water is then sufficiently de-aired for use in the triaxial apparatus.

The purpose of de-airing is to make the water as incompressible as possible. Using de-aired water in the cell and pressure controllers means that changes in the specimen during preparation and testing are all due to soil properties, rather than some being due to the compression of air in the water.

4. Specimen Preparation and Testing Procedure

The procedures and techniques used to prepare and test a soil specimen greatly influence the results gained from triaxial testing. For example, the way a soil is reconstituted into a mould has a direct effect on the fabric created for that specimen. The end conditions on a specimen (such as having either friction or no friction) will affect the way the specimen deforms during the application of load. Factors such as these have been considered and different methods tried during the testing period from July 2006 through to February 2007. The procedures outlined below have been determined to currently be the best methods for preparation and testing as of June 2007. They have been used since February 2007 in the testing of silty sand.

4.1 Specimen Preparation

There are a number of ways to prepare a specimen for triaxial testing. The current research has used a split mould with membrane placed on a removable pedestal as the overall specimen mould. The silty sand used in testing has then been moist-tamped into this mould to create the specimen. A more detailed procedure for doing this is outlined below.

4.1.1 Mould preparation

GDS Instruments supplied a number of items with the overall triaxial testing apparatus package. These included split moulds, membranes, pedestals, top-caps, porous stones and o-rings. These are shown below in Figure 13.

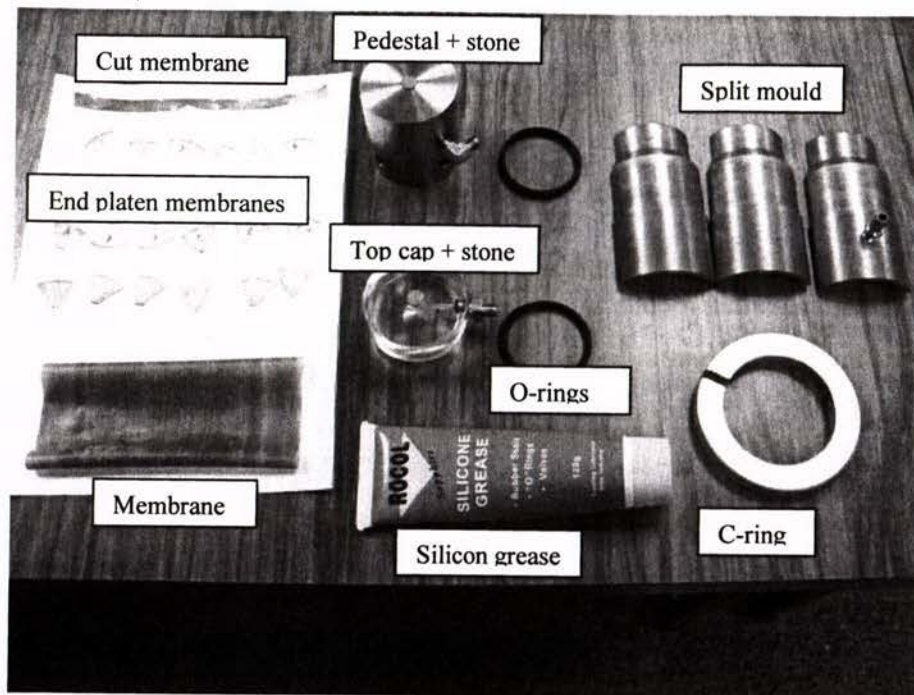


Figure 13 – Gear used for triaxial testing.

The size of the test specimens were set at a standard 50mm diameter by 100mm high. It was also decided that enlarged end platens were to be used – a base pedestal and top-cap with surface diameters of 60mm to allow uniform deformation of a specimen in the radial direction. The split mould had a groove placed around the inside, and a tap attached to allow a vacuum to hold the membrane to the split mould. Membranes were also cut up to create four sets of end platen surfaces. These were each circular in shape with a 50mm diameter (including a central hole for the porous stone) before being cut into six equal segments. The whole setup procedure is described below:

- Place silicon grease all over the end platen of the base pedestal. Take one layer (6 segments) of end platen membrane surfaces (pre-greased) and place on the pedestal, creating a base layer. Then place the next layer (no grease) on top of the first layer carefully, covering the gaps in the base layer. This allows the layer in contact with the sample to move over the base layer as the sample deforms. Repeat this step for the top-cap.

- Grease around the outside of the pedestal from the end platen to the location of the valve. This helps to stop water from the cell moving under the specimen membrane and into the specimen. Repeat this for the top-cap, except covering all sides of the top-cap. Set aside.
- Take the specimen membrane (pre-marked) and place over the pedestal, up to the first 30mm mark and align correctly. Use a thin piece of cut membrane to wrap around the base of the membrane. Then take two o-rings and place them over the membrane and pedestal, securing the membrane to the pedestal near the membrane base. These measures also help to prevent water leaking into the specimen.

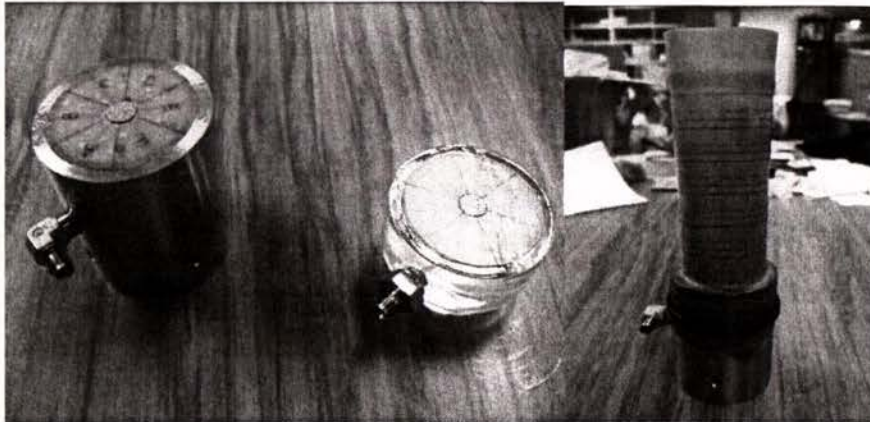


Figure 14 – Pedestal and top-cap greased with end platen membrane surfaces in place (left). Membrane secured to pedestal with o-rings and cut membrane (right).

- The pedestal/membrane, top-cap and two other o-rings are now placed on a tray and weighed. This allows a specimen void ratio to be calculated post-test.
- The split mould is placed outside the membrane, so that it sits on top of the membrane and pedestal. The c-ring is taken and put around the mould, so that it sits as high on the mould as possible. Two pieces of masking tape are then used to wrap around the mould below the c-ring. One of the remaining two o-rings is placed over the mould, above the c-ring. The other is placed inside the mould (sitting loosely at the top) and the whole mould setup is weighed.

- The loose o-ring is removed, and a vacuum of around 20kPa is applied. The membrane sticking out above the mould top is then folded back over the outside of the mould up to the top mark on the membrane, and adjusted correctly. The loose o-ring is then placed over the folded membrane, securing the membrane to the split mould. A tube is then attached from the vacuum to the mould, applying a vacuum pressure of around 20kPa. This holds the membrane against the sides of the split mould. The mould is now ready for sand placement.



Figure 15 – Mould setup ready for sand placement.

4.1.2 Soil Reconstitution

It was decided that moist-tamping would be the best method for the silty sand reconstitution. This is due to moist-tamping enabling relatively loose specimens to be created, as well as minimising the segregation of particles (sand and silt) during placement. The method for this moist-tamping is outlined below:

- The membrane is pre-marked using a permanent marker, splitting the main height of soil placement (95mm) into 6 equal layers (approximately 15.8mm each). This is done for 95mm as the membrane needs to be stretched when folding over the

mould, bringing the total height to 100mm. Guidelines are also placed at 4mm and 8mm above each of the layer lines for use during tamping.

- A paper funnel is placed on the scales, and the required soil weight for one layer (one sixth of the total required for the specimen) is placed in the funnel. This soil is then poured into the mould, and mixed carefully with a small screwdriver to spread the soil out.

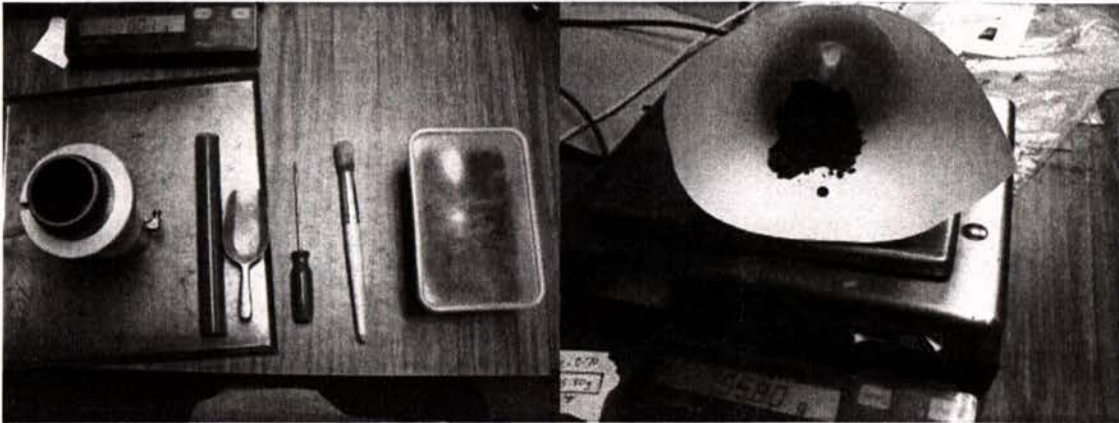


Figure 16 - From left to right: mould, plastic tamper, soil scoop, screwdriver, brush, soil container (left). The soil sitting in the paper funnel on the scales (right).

- The layer is tamped using a 25mm diameter by 203mm high plastic rod. This is done by firstly pressing the layer down gently, then tamping around the outside of the specimen in a clockwise direction until reaching the initial start point ($0^{\circ}/360^{\circ}$). This should take around 10 – 12 tamps whilst using a reasonable level of force. The next phase of tamps should be done starting at the horizontally opposite point (180°), and in the anti-clockwise direction. The remaining two phases of tamps should be done in a similar way (one clockwise, one anti-clockwise) starting at 90° and 270° . With all four phases done, the central region should be lightly tamped around 10 times. This now completes a set of tamps. These sets should be repeated as per necessary depending on the targeted density of the specimen. When finished, the layer surface is lightly scratched in lines at around 4 – 5mm spacing using the small screwdriver. This should be done in two perpendicular directions to create a cross-hatch pattern.

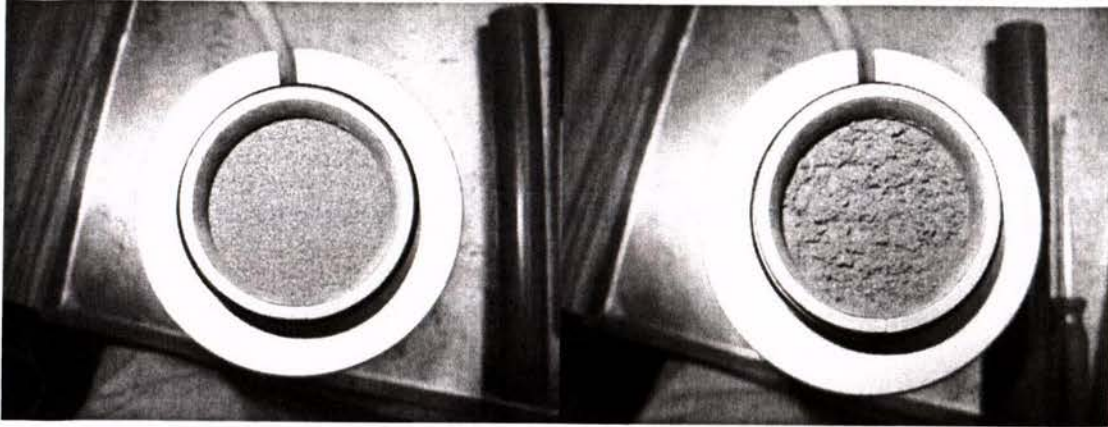


Figure 17 – Soil layer after end of tamping (left). Soil layer after tamping and scratching (right).

- This tamping method is repeated for the first 5 layers. The sixth layer requires an extension mould (50mm diameter) to be sat on top of the specimen mould, allowing the final layer to be tamped to the top of the specimen mould. Guidelines are also marked on the extension mould. Once the soil has been placed and tamped to approximately the right height, the extension mould is removed. The specimen can then be tamped gently by eye to obtain a flat top surface. The vacuum is then turned off, and any sand particles around the edges of the mould are brushed away.
- The specimen is now weighed to allow the mass of sand added to the mould to be calculated. The o-ring placed over the folded membrane is removed, and then placed back on the mould below the location of the membrane, next to the other o-ring. The specimen is now ready to be placed into the triaxial cell.

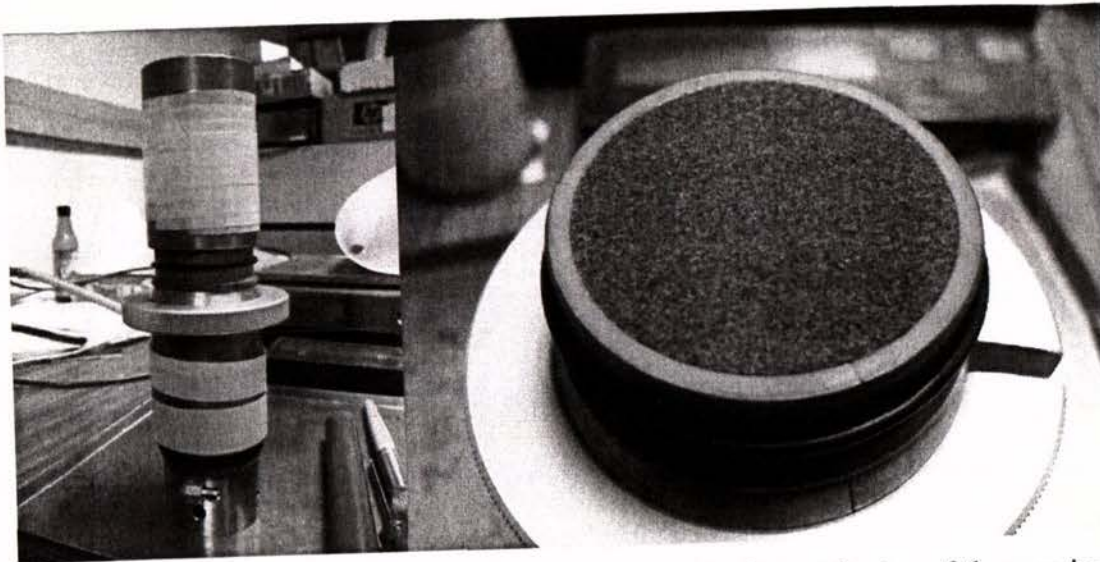


Figure 18 – Mould with extension mould on top (left). Surface at the top of the specimen (right).

4.2 Testing Preparation

The triaxial testing preparation currently used involves placing the specimen in the triaxial cell, stabilising it by vacuum when removing the mould, filling the cell with de-aired water, saturating the sand, and finally consolidating the specimen. A more detailed explanation of this preparation is outlined below:

- Once the specimen has been prepared as detailed in the Soil Reconstitution section, the specimen is placed into the triaxial cell and locked in place. This is done by placing the pedestal onto the axial ram, and tightening the pedestal to the ram through the use of a key.
- The top-cap is now taken and the docking sleeve placed over it. The top-cap and sleeve are then placed in the cell, between the top of the specimen and the bottom of the docking-cap. They are then pushed up so that the top-cap is in hard contact with the docking-cap, and the sleeve is located around the outside of the docking-cap. The exit valve on the docking-cap is closed by placing a

screw-cap on the valve and tightening. This holds the top-cap and sleeve to the docking-cap through pressure considerations.

- The c-ring is removed from the mould, shifting it between the top-cap and the specimen top. The mould is now held in place by the masking tape. The specimen is then moved upwards using the motorised cell control box, until the top-cap and specimen membrane are in contact.

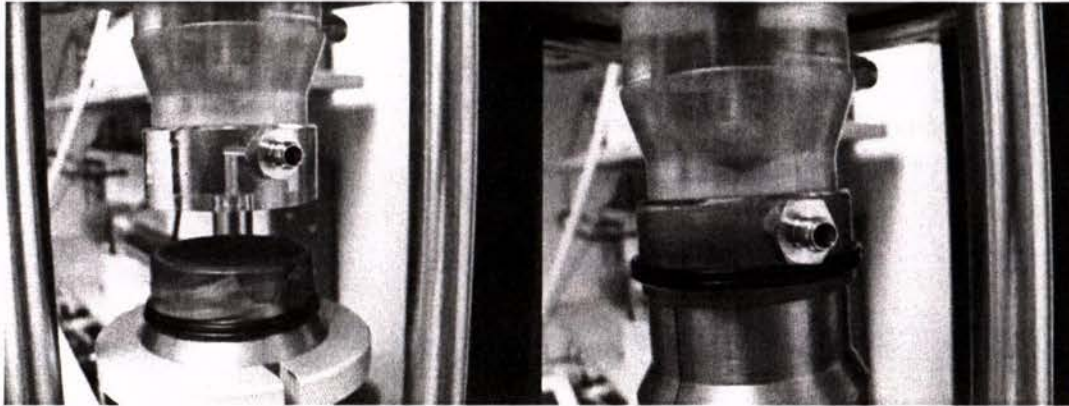


Figure 19 – The specimen with the top-cap and sleeve in place (left). The specimen with the top-cap in place and the membrane folded up over the top-cap (right).

- The folded part of the membrane can now be rolled up onto the outside of the top-cap. This should be done as to not rip or puncture the membrane. The two o-rings sitting on the mould can also be rolled up onto the top-cap, securing the membrane to the top-cap. This helps prevent cell water from penetrating the specimen from the top.
- Grease the valves of the pedestal, top-cap, and internal back pressure entry and exit valves. Take one internal tube and connect one end to the top-cap valve and the other to the back pressure exit valve, tightening each. Now take another tube and connect to the pedestal valve and back pressure entry valve. This allows back pressure water to enter the specimen from the base, flow up through the sand, and exit out the top-cap. At this point the axial load should be set to target 0kN.

- Attach a tube to the external back pressure entry valve and close all other valves that connect to the specimen. Connect the other end to a vacuum pump, and apply around 20kPa of vacuum. The masking tape around the mould can then be removed, along with the mould itself, as the vacuum will hold the specimen together. At this point the diameter of the specimen can be measured at five different locations. Finally the two o-rings around the base pedestal can be rolled up so they are just below the top of the pedestal. Care should be taken not to roll them onto the specimen itself. The cell can now be closed and tightened.

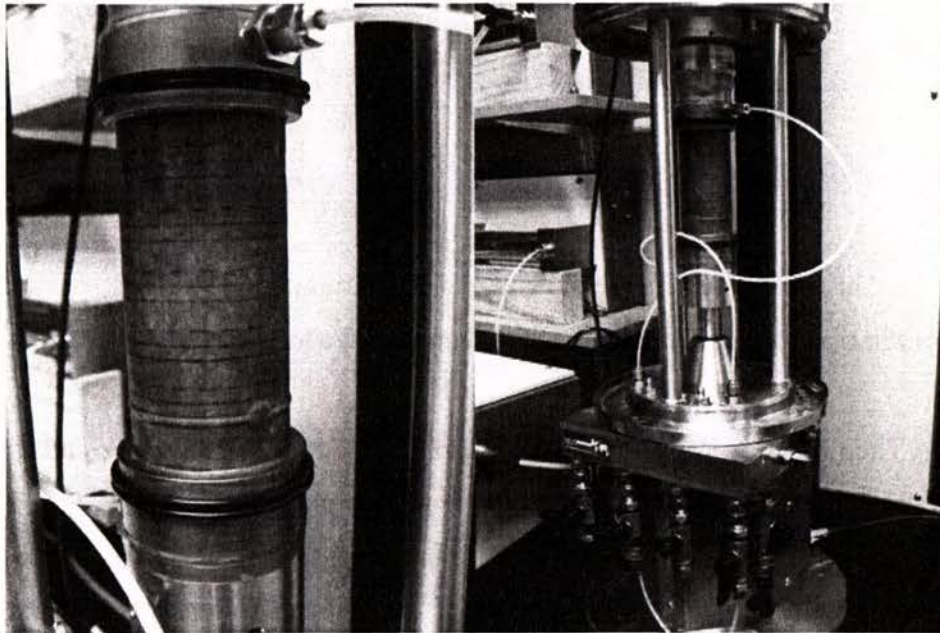


Figure 20 – Specimen with split mould removed and o-rings rolled up (left). Specimen and tubing in place in the triaxial cell (right).

- De-air enough water to fill the triaxial cell. Place this into a sealable container and place the container above the triaxial cell. Connect a tube between the container tap and the cell, so that the de-aired water can flow into the cell (around the outside of the specimen). Let this fill.

- While the cell is filling, place some de-aired water into a beaker and turn on the cell pressure controller. Place the cell pressure controller tube into the beaker and fill the controller. Once filled, hold the end of the tube in line with the specimen mid-height, and zero the pressure. Now connect to the cell and empty a small amount of the controller water. This helps to remove any air bubbles in the valve between the controller tube and the opening into the cell chamber.

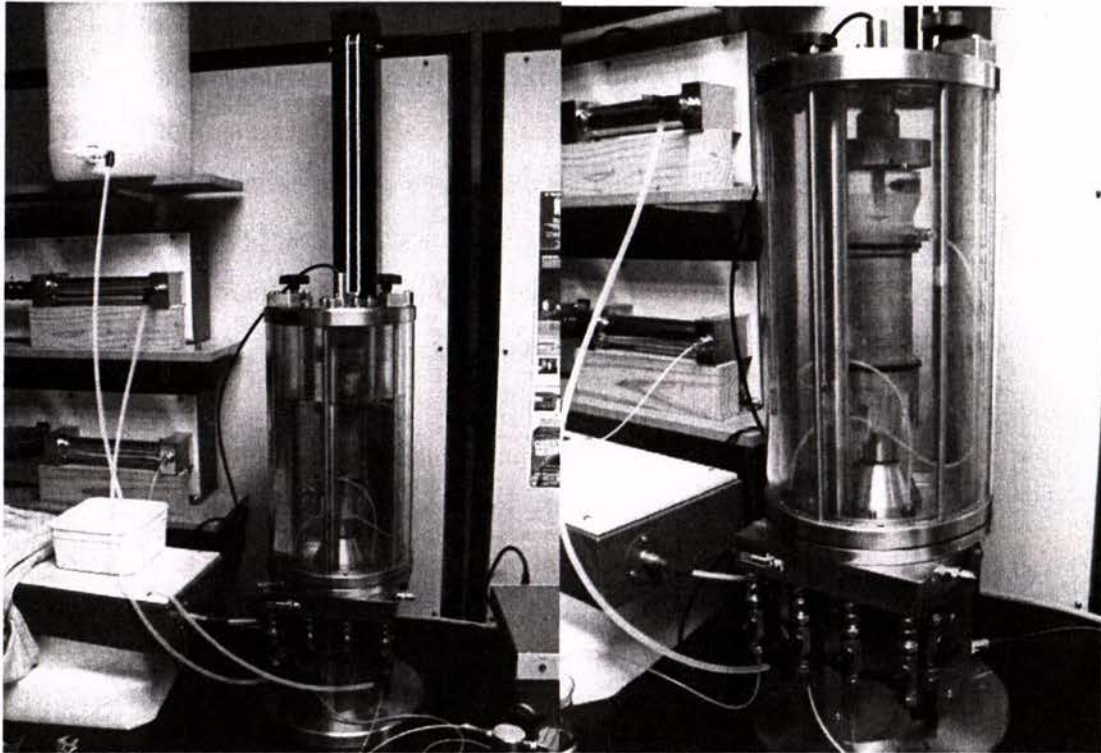


Figure 21 – Triaxial cell with specimen inside filling with de-aired water from container (left). The triaxial cell full with the de-aired water tube removed (right).

- Once the cell has filled, secure the top exit valve of the cell by placing the screw-cap and tightening. This means the cell system is no longer in contact with atmospheric pressures. The PC should be set to a Triaxial Acquisition test stage with data logging only (using the GDSLab software), and the axial displacement set to zero. A cell pressure of 15kPa can now be targeted using the cell pressure controller, with the axial load again set to target 0kN.

- With the cell pressure close to 15kPa, the vacuum can be removed from the specimen, and the back pressure entry valve closed. The cell pressure is then re-targeted to 30kPa using the controller.
- A tube is used to connect the bottle of CO₂ with the back pressure entry valve. The CO₂ flow is begun before making this connection, with a very low pressure. Another tube is connected to the back pressure exit valve and placed in around 100mL of de-aired water in a beaker. The entry and exit valves are then opened, allowing CO₂ flow from the bottle, up through the specimen, and out through the exit valve into the de-aired water. The pressure of flow is then adjusted until around 3 – 4 bubbles per second are appearing in the water. This percolation of CO₂ helps to improve saturation of the specimen, as it replaces the air in the specimen and is more soluble in water than air. The system should be left for 2 hours of CO₂ percolation.
- Once CO₂ percolation has finished, remove the tubes and fill the back pressure controller with de-aired water in the same way as the cell pressure controller was filled. When filled, zero the volume reading as well as the pressure, in the same way as for the cell pressure controller (to specimen mid-height). Then attach the back pressure tube to the back pressure entry valve on the triaxial cell.
- Set the back pressure controller to run a volume ramp function, whereby the de-aired water is percolated through the specimen at a constant rate. The current research has used a rate that percolates approximately 190mL in 7 hours. The test should be checked in the early hours of this percolation to make sure no blockages in the line or porous stones cause a fatal (liquefying) rise in specimen pore pressure. Once the first cycle of percolation is complete, the back pressure controller is re-filled and a second cycle is run.

- With water percolation complete, re-fill the back pressure controller to around half-full, zero the volume reading, and reconnect to the back pressure entry valve. Use an Advanced Loading test stage to ramp the cell and back pressures to test values (usually 200kPa and 100kPa respectively) over 60 minutes, with a constant deviator stress of 0kPa. Before starting this stage, make sure the back pressure entry valve is open, and the exit valve is closed. Set another stage to run directly after the first, target constant test pressures and a deviator stress of 0kPa. Leave the tests to run until specimen consolidation has occurred (this was around 4 – 5 hours for the current research).
- Once specimen consolidation is complete, run a B-check on the specimen. This checks the saturation of the specimen. Raise the cell pressure by 2 – 3kPa whilst holding the back pressure constant, and the deviator stress at 0kPa. A value of $B \geq 0.95$ is usually required for satisfactory saturation. Once checked, re-target a cell pressure of 200kPa, back pressure of 100kPa, and deviator stress of 1kPa. This is done to ensure proper specimen loading from the beginning of a loading test. Leave this for around 5 minutes to stabilise. The specimen is now ready for the loading test to begin.

4.3 Specimen Loading

This research is currently performing two types of test loadings: undrained monotonic loading and undrained cyclic loading. Undrained testing involves allowing no volume change in the specimen whilst being loaded. This lets changes in the specimen pore pressure (back pressure) occur.

4.3.1 Monotonic Loading

The monotonic loadings carried out during the current research have been completed by increasing the axial strain of the specimens at a constant rate (strain control). The rate

used is 0.3mm/min, giving an axial strain of 10% every 33.3 minutes. This rate was chosen based on other research (Verdugo 1992), (Zlatovic 1994) using sands with similar silt contents. This loading regime is set in GDSLab by targeting a constant cell pressure, holding back volume constant, and using the ramp function to target an axial displacement in a set amount of time (giving a rate). Tests were generally continued until specimen liquefaction occurred (zero effective stress) or until around 40% axial strain was reached.

4.3.2 Cyclic Loading

The cyclic loadings carried out during the current research have been completed by oscillating the deviator stress of the specimens at a constant time period (stress control). The rate used for one sinusoidal stress cycle is 2min/cycle, with the specimen being subjected to the full range of required deviator stress in this time. This rate was chosen based on the number of data points that were desired for a cycle (GDSLab logs a point about every 3 seconds – this gives around 40 points per cycle). This loading regime is set in GDSLab by targeting a constant cell pressure, holding back volume constant, and using the sinusoidal function to target a deviator stress value about a datum (0kPa) over a cycle time period. Tests were generally run until a couple of cycles after specimen cyclic liquefaction occurred (zero effective stress).

4.4 Post-test Procedure

A post-test procedure was developed for the current research to enable a secondary specimen void ratio calculation. Once loading has finished, the back pressure entry valve is closed. The cell pressure is lowered back to 0kPa and the cell top exit valve is opened, bringing the cell water back to atmospheric pressure. The cell water is drained and the cell is unscrewed and lifted up. The following procedure is then used:

- The specimen is left in place and dried as much as possible using paper towels. It is important to carefully soak up any water located around the o-rings.
- The docking-cap exit valve is opened, and the top-cap/sleeve is carefully pulled away from the docking cap, leaving the specimen with no top support. The sleeve can then be taken off the top-cap.

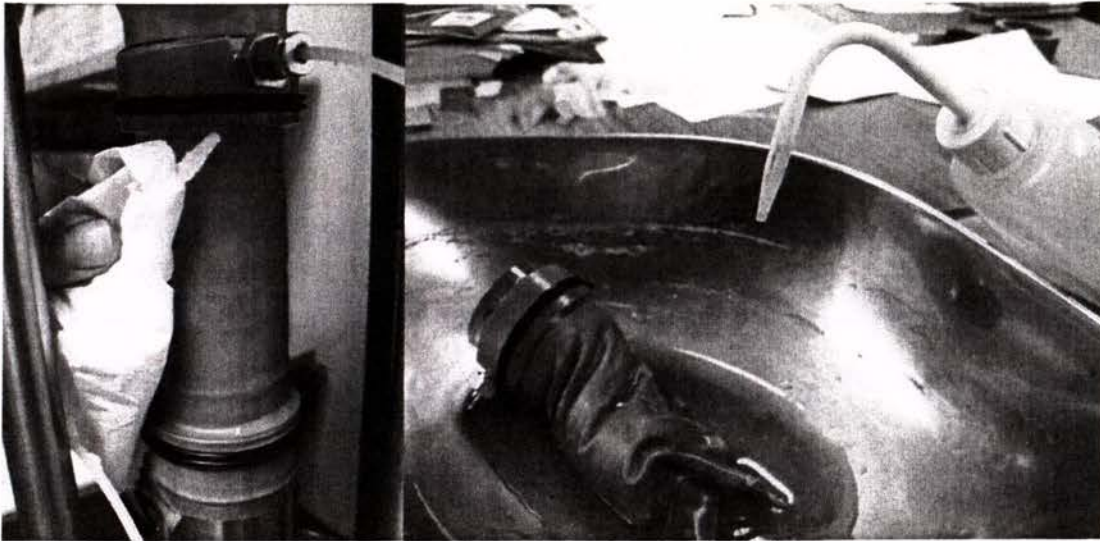


Figure 22 – Drying of the specimen after the cell chamber has been lifted (left). Washing out the specimen into the oven-proof dish (right).

- The pedestal is loosened and removed from the cell, still with the internal tubes connected. It is placed with care on a tray right beside the cell, and final drying of the specimen can take place. It helps to remove the thin piece of cut membrane from around the membrane base to completely dry the specimen.
- A large oven-proof dish is weighed without anything inside. The dish is then placed on under the specimen on the tray, so that the specimen sits inside the dish. The internal tubes are then disconnected from the top-cap and pedestal. The dish is weighed straight away, giving a combined weight of the dish and specimen with the same amount of water and sand as during test loading.

- The specimen is disassembled in the dish, making sure not to loose any sand or water. This is done by removing the membrane from the base pedestal, removing the top-cap, and washing out the parts using water washing bottle. This process should be done with care, making sure to remove and wash such things as the end platen membrane surfaces form the top-cap and pedestal. This leaves the majority of sand in the dish with an unknown amount of water. The dish is then placed in a drying oven.
- Once the water has evaporated form the dish (it is generally left to dry for 24 hours) the dish is weighed. The mass of sand can be determined, and using the other recorded masses and sand properties, a specimen void ratio calculation during test loading can be made.

5. Albany Sand Triaxial Tests (Apparatus Verification)

A number of triaxial tests were initially carried out using Albany Sand to enable verification of the new apparatus. This was done in conjunction with a 3rd Professional Project. The testing included drained monotonic loading, undrained monotonic loading, and undrained cyclic loading. The test preparation procedure was not constant during this testing phase as a number of issues were still being solved and new methods being tried. This meant that although over 25 specimens were created in this testing phase, only 13 gave results that were considered useful. These tests did however help to show that the new apparatus was working correctly and would be suitable for further research use.

5.1 Drained Monotonic Triaxial Testing

Two drained monotonic tests were carried out using Albany Sand (Test 1 and Test 2). The specimens were both created using a dry pluviation sand placement technique (as opposed to moist tamping). This was done by funnelling sand into the mould in three layers. Each layer was then tamped around 50 times. Both specimens were isotropically consolidated (the external specimen pressures were increased at the same rate in both the axial and radial directions). The tests were strain-controlled (constant strain increase). A summary of the specimen properties from each test is shown below in Table 1.

Table 1 – Drained monotonic test specimen properties.

Test Number	1	2
Estimated Test Void Ratio (e_{test})	0.644	0.645
Estimated Test Relative Density ($D_r\%$)	62 %	62 %
Skempton's B-Value	0.95	0.95
Cell Pressure	200 kPa	250 kPa
Back Pressure	100 kPa	100 kPa

Effective Confining Stress (p')	100 kPa	150 kPa
Axial Displacement Rate	0.05 mm/min	0.05 mm/min
Estimated Final Void Ratio (e_{final})	0.733	0.724

Note that in Table 1 the B-values are both calculated to be 0.95. This means the specimens were sufficiently saturated before application of load. Effective confining stresses (p') of 100kPa and 150kPa simulate soil pockets in the ground of approximately 10m and 15m respectively. Also note that as the tests were drained, the cell and back pressures were kept constant throughout loading. The specimen deformation for Test 1 can be seen in Figure 23. Test 2 showed very similar deformation.

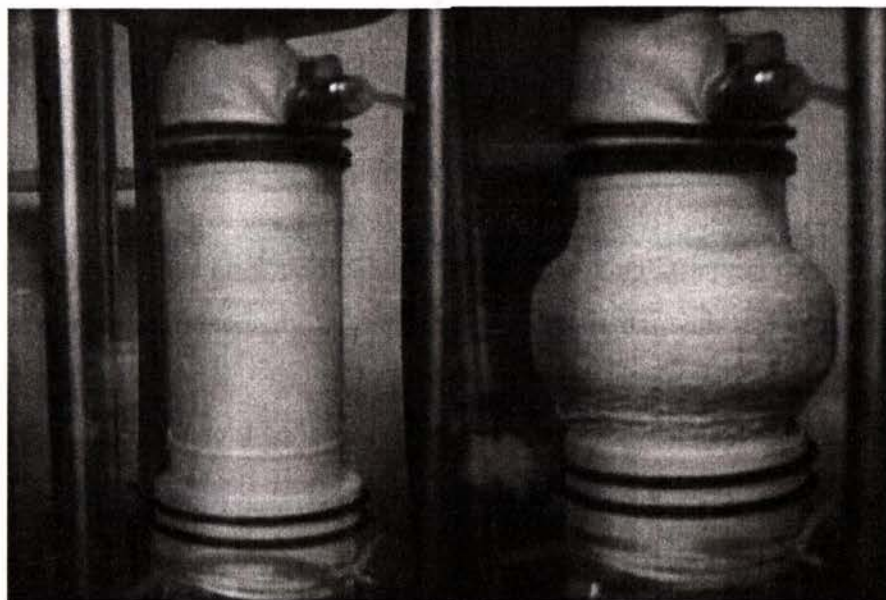


Figure 23 – Test 1 specimen at 0% axial strain (left) and at 36% axial strain (right).

Note the barrelling of the specimen at large axial strain (36%). This is due to the end platens having no membrane surfaces to allow for movement, and the ratio of specimen dimensions (height twice the diameter). The stress-strain behaviour of the specimens is shown below in Figure 24.

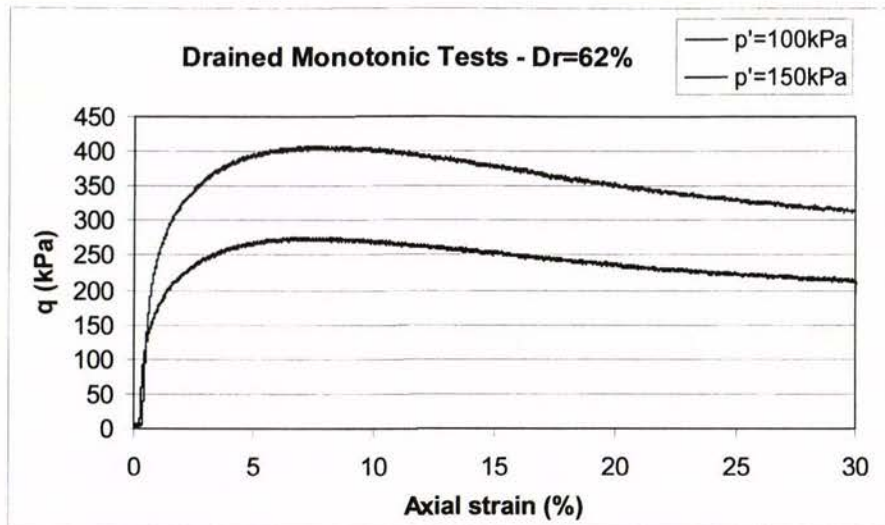


Figure 24 – Stress-strain behaviour of Test 1 and Test 2. The deviator stress (q) is plotted against the axial strain.

Figure 24 shows the deviator stress response of each of the specimens to a constantly increasing axial strain. Both tests reach a peak strength, then experience strain softening before reaching a steady state (constant q with increasing axial strain). Test 1 specimen ($p' = 100\text{kPa}$) shows a smaller peak strength than the Test 2 specimen ($p' = 150\text{kPa}$). This is expected, as a larger confining stress tends to result in a higher peak strength for clean sand specimens of the same initial density during drained loading. This can be accounted for by normalising the deviator stress by the effective confining pressure. This is shown below in Figure 25.

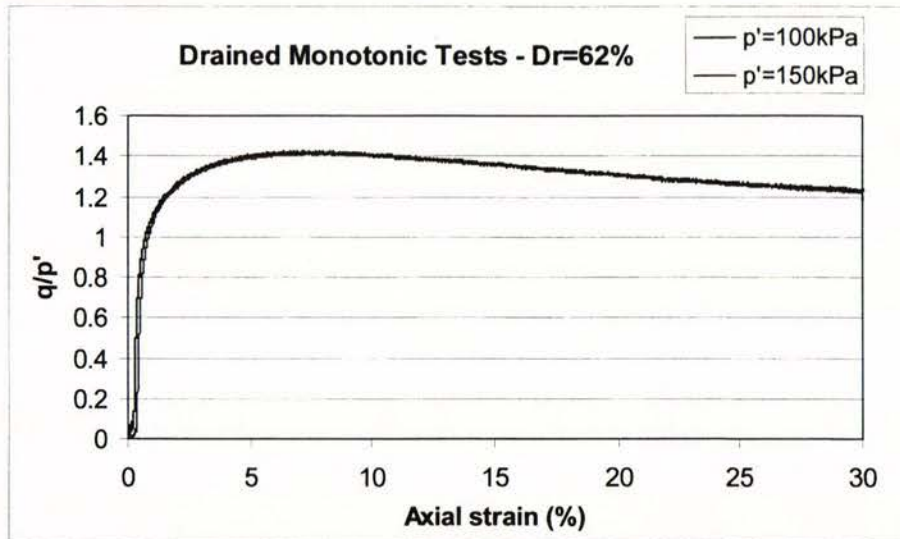


Figure 25 – Stress-strain behaviour of Test 1 and Test 2. The deviator stress (q) is normalised by the test effective confining pressure (p').

Normalising q by p' shows the curves collapse onto each other. It also shows that q/p' is constant at steady state for the Albany Sand. This can be used to determine the friction angles for the sand using Mohr-Coulomb failure criterion.

Table 2 – Friction angles of Albany Sand (Roper 2006).

<u>State</u>	<u>Friction angle ϕ</u>
Peak State	33
Steady State	31

The friction angles of a soil are widely used in engineering design. In particular, they are very important in determining the stability of slopes and foundations.

As the tests were drained, a volume change in the specimens was recorded during loading (change in specimen pore water volume). This is due to the specimen either contracting or dilating as the axial strain is increased to maintain a constant back pressure of 100kPa. This behaviour is shown below in Figure 26.

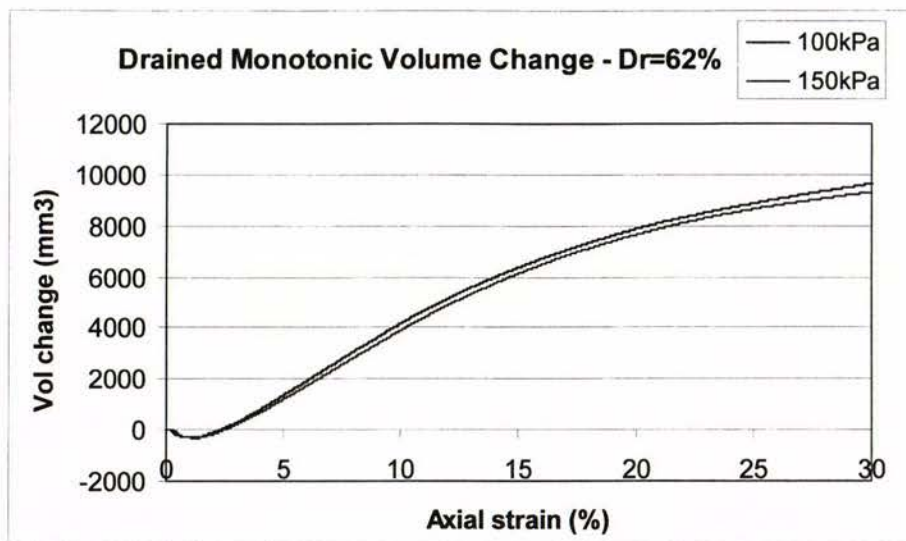


Figure 26 – Volume change of Test 1 and Test 2. The volume change is shown in mm³ (1mL = 1000mm³).

The volume change plot shows an initial contraction of the specimens (a negative change implies water leaving the specimen). This initial contraction is then suppressed by a greater dilative tendency. This is very typical of a medium-dense specimen of clean sand being subjected to drained monotonic loading.

5.2 Undrained Monotonic Triaxial Testing

Two undrained monotonic tests were carried out using Albany Sand (Test 3 and Test 4). The specimens for these tests were created using two different sand placement techniques. Test 3 used dry pluviation in the same way as for the drained monotonic tests (Test 1 and Test 2). Test 4 used a moist tamping sand placement technique. The Albany Sand was mixed with water to obtain a moisture content of 5%, and was placed in four layers into the mould. Each layer was tamped 15 times. This created a very loose specimen (low density). Both specimens were isotropically consolidated. The tests were strain-controlled (constant strain increase). A summary of the specimen properties from each test is shown below in Table 3.

Table 3 – Undrained monotonic test specimen properties.

Test Number	3	4
Estimated Test Void Ratio (e_{test})	0.660	0.877
Estimated Test Relative Density ($D_r\%$)	57 %	-16 %
Skempton's B-Value	0.95	0.98
Cell Pressure	400 kPa	250 kPa
Back Pressure	100 kPa	100 kPa
Initial Effective Confining Stress (p')	300 kPa	150 kPa
Axial Displacement Rate	1.0 mm/min	1.0 mm/min

Note that Test 4 gave a relative density $D_r = -16\%$. The values of e_{max} and e_{min} (both used in calculating D_r) were taken from previous laboratory work done at the University of Canterbury (Chambers 2000). It is therefore likely that these values were not fully accurate for the tested batch of Albany Sand. This is not an issue however that has major impact on the other results (the value of specimen void ratios are still correct). Also, the axial displacement rate for the loadings was increased to 1.0mm/min due to the undrained condition.

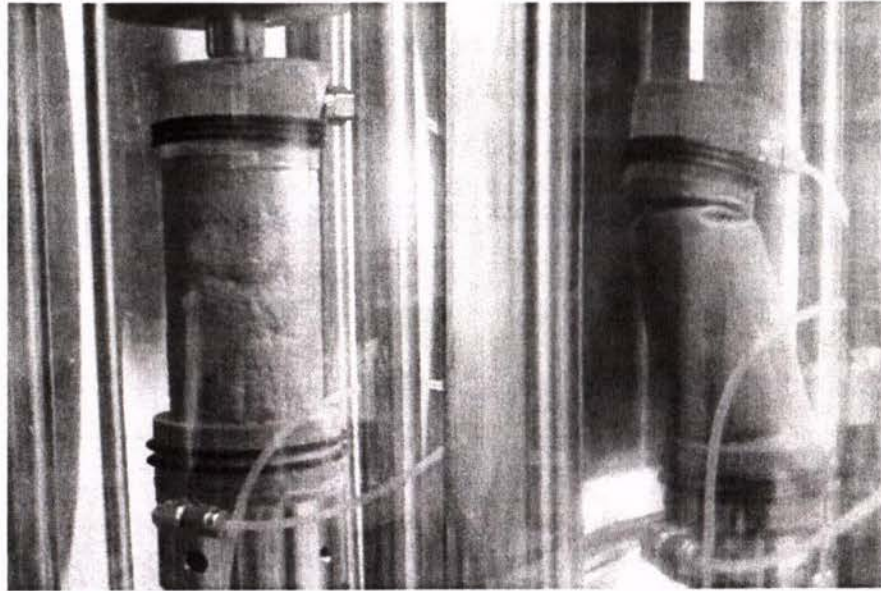


Figure 27 – Test 4 specimen at 0% axial strain (left) and after liquefying (right).

Figure 27 shows the deformation of the Test 4 specimen, which liquefied during undrained monotonic loading. As can be seen, the specimen is vertical and solid before application of strain. Liquefaction then causes the specimen strength to be lost, and once the cell pressure is removed the specimen cannot support its own weight. This simulates the field phenomenon of flow liquefaction in the laboratory. If this was to happen in (for example) a steep sandy-soil slope, the slope would incur very large deformations due to the lack of material strength.

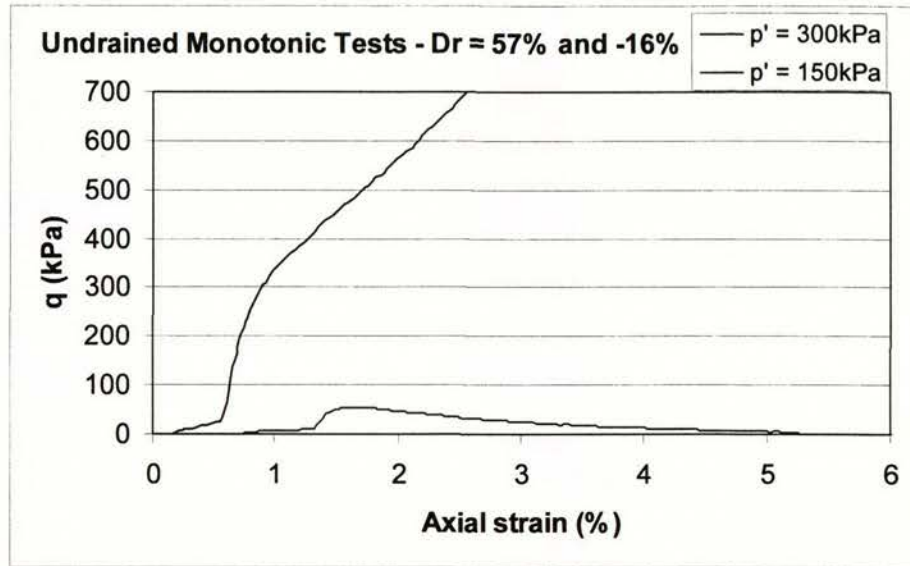


Figure 28 – Stress-strain behaviour of Test 3 and Test 4. The deviator stress (q) is plotted against the axial strain.

Figure 28 shows two very different behaviours. Test 3 ($p' = 300\text{kPa}$) shows strain hardening, and reaches the apparatus load limit (2kN or 1000kPa for a 50mm diameter specimen) before reaching steady state. This is highly dilative behaviour. Test 4 is the opposite – the specimen reaches a peak strength, then experiences strain softening. This continues and the specimen liquefies, as the soil strength (q) has dropped to zero. This means that the specimen now has no resistance to applied load, and can deform very easily. This is highly contractive behaviour. These two tests show the large difference density plays in the behaviour of clean sand during undrained loading.

Note that both tests experience a significant amount of strain before the stress begins to fully increase. This was an issue associated with the docking of the specimen to the top ram of the cell. The problem meant the specimens were not in full contact with the ram when loading was begun, creating a small increase in deviator stress with up to 1.5% axial strain. This issue was eliminated with further test procedure development.

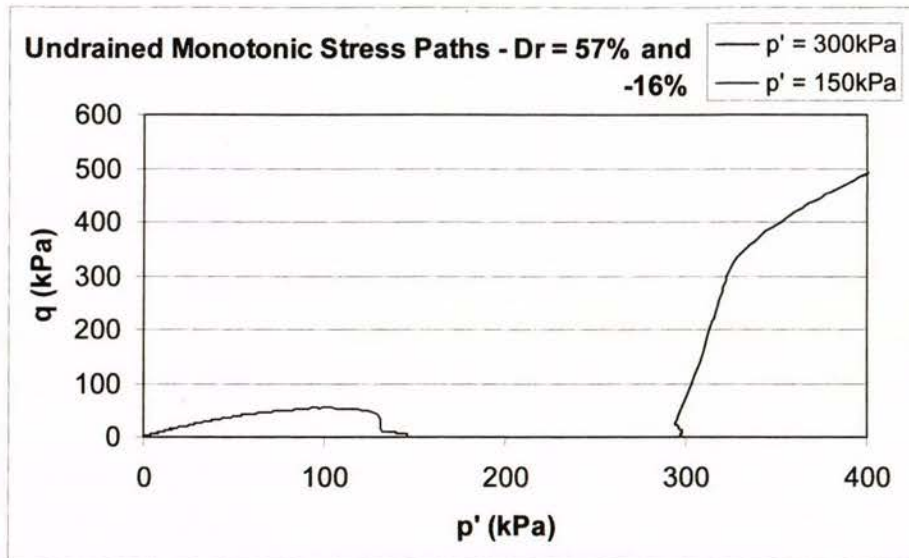


Figure 29 – Undrained stress paths of Test 3 ($p' = 300\text{kPa}$) and Test 4 ($p' = 150\text{kPa}$). The plot has cut out the extension of the Test 3 stress path.

Figure 29 shows the undrained monotonic stress paths for each of the tests. The effective confining stress p' changes during loading due to the undrained condition. Test 3 shows highly dilative behaviour, which reduces the pore pressure within the specimen. This reduction in pore pressure causes p' to increase. The increasing deviator stress is another reason for an increasing p' , as the application of axial stress further confines a specimen. Test 4 shows highly contractive behaviour, which increases the pore pressure within the specimen. This increase causes p' to decrease, and eventually reach $p' = 0\text{kPa}$. This is flow liquefaction, as the pore pressure has reached the same value as the cell pressure. This means that the internal and external pressures acting on the specimen are equal, and load is not being carried by the specimen.

The undrained testing of clean sands is highly important to engineering design, as it simulates the behaviour of a saturated sand deposit subjected to a sudden load. Examples of this are an earthquake or an explosive blast. The soil deposit does not have time to drain due to the speed of the loading – this means pore pressure will either increase or reduce until it has time to dissipate. As shown by the undrained monotonic tests, an

increasing pore pressure can result in a total loss of soil strength. This can have major implications in the field, such as the slope instability described above.

5.3 Undrained Cyclic Triaxial Testing

Nine undrained cyclic tests were carried out using Albany Sand. Four of these are outlined below (Tests 5 – 8), as they gave the most consistent results. The initial three cyclic tests attempted to evaluate a liquefaction curve for Albany Sand, however the specimen densities had too much variation. The final two cyclic tests were used to calculate stiffness properties. This should be done using one test, but a specimen docking problem in the first test meant a second test was required.

Four specimens were created using a moist tamping sand placement technique to evaluate a liquefaction curve for the Albany Sand. The sand was mixed to a moisture content of 5 – 6%, and deposited into the mould in 5 layers. Each layer was tamped 50 times, with an extra 25 light tamps on the top specimen layer. All specimens were isotropically consolidated. The tests were stress-controlled (sinusoidal oscillation of the deviator stress q) with an oscillation period of 3 minutes. A summary of the specimen properties from each test is shown below in Table 4.

Table 4 – Undrained cyclic test specimen properties.

Test Number	5	6	7	8
Estimated Test Void Ratio (e_{test})	0.725	0.722	0.732	0.723
Estimated Test Relative Density ($D_r\%$)	35 %	36 %	33 %	36 %
Skempton's B-Value	0.98	0.98	0.97	0.98
Cell Pressure	200 kPa	200 kPa	200 kPa	200 kPa
Back Pressure	100 kPa	100 kPa	100 kPa	100 kPa
Initial Effective Confining Stress (p')	100 kPa	100 kPa	100 kPa	100 kPa

Applied Cyclic Stress ratio (T = 3mins)	0.100	0.200	0.150	0.125
--	-------	-------	-------	-------

Note from Table 4 that all tests were almost identically prepared. The only significant difference is the CSR (Cyclic Stress Ratio) applied to each of the specimens.

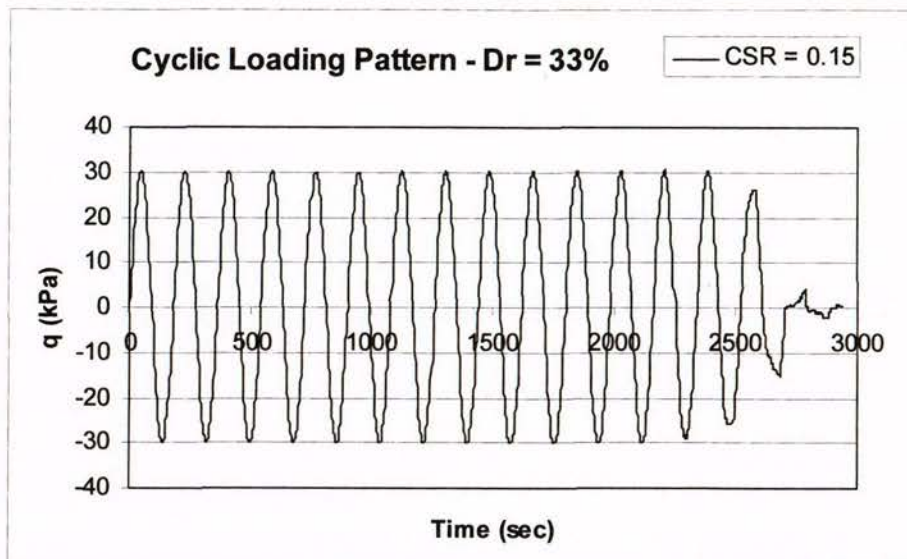


Figure 30 – Cyclic loading pattern for Test 7 (CSR = 0.15).

The CSR is defined as the single amplitude stress peak divided by twice the initial effective confining stress, p' . In Figure 30 the single amplitude stress is 30kPa, the initial p' is 100kPa, and therefore the CSR = 0.15. This means that the specimen is subjected to a deviator stress of +30kPa (compression) and -30kPa (extension) every cycle.

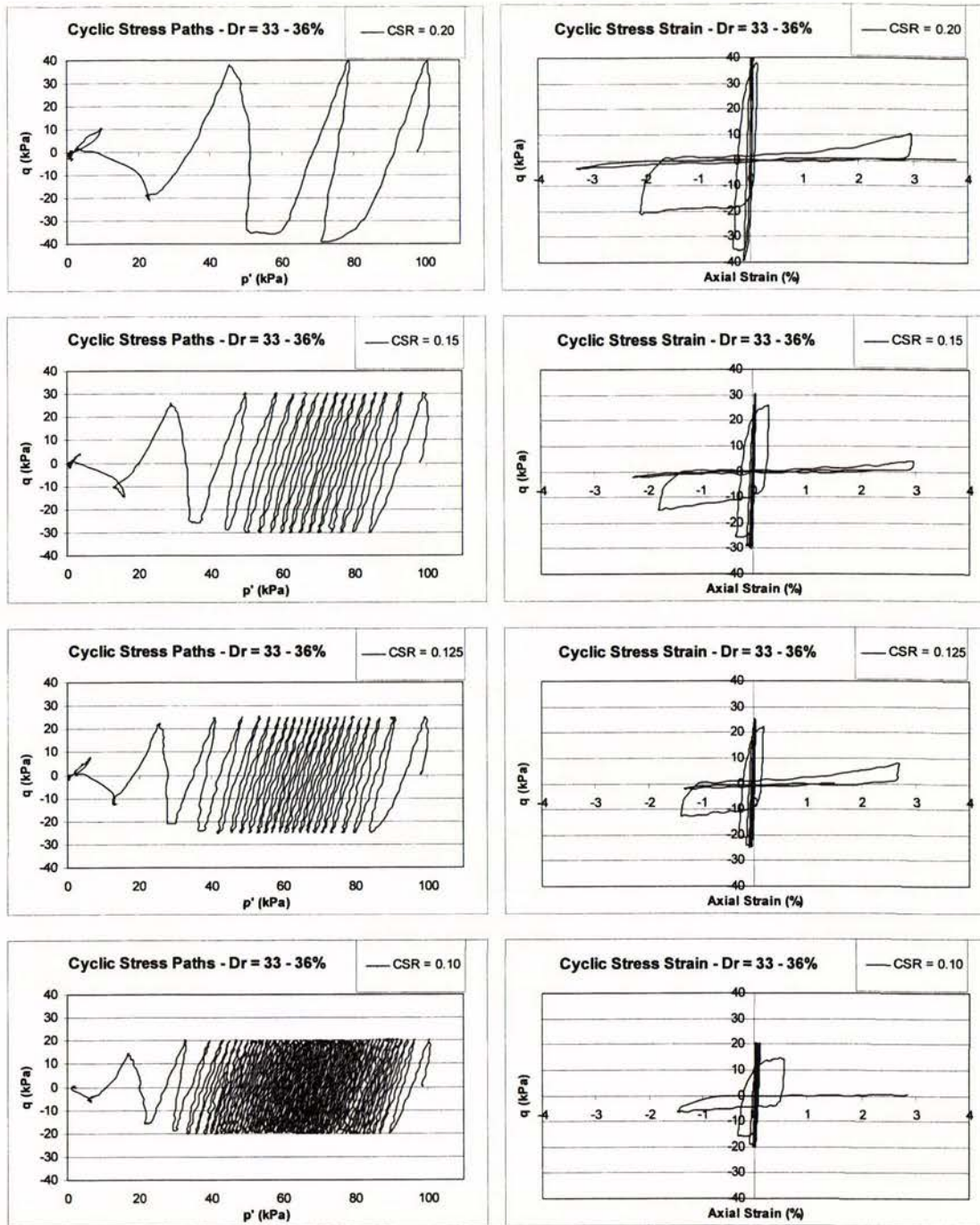


Figure 31 – Cyclic stress paths and cyclic stress-strain paths for Tests 5 – 8.

Figure 31 shows (left-hand side) the cyclic stress paths for the undrained cyclic tests. This clearly displays the effect of varying CSR. The effective confining stress decreases during each of the tests, and is common to all cyclic testing. This is due to pore pressure

build-up in the specimens due to the repeated cycling of stress and the undrained test condition. This rate of pore pressure build-up varies with changing CSR – a larger CSR causes faster build-up (for specimens of similar state). This leads to a faster decrease in the effective confining stress, and less cycles required to reach $p' = 0\text{kPa}$. For example, in Figure 31 the specimen subjected to a CSR = 0.20 (Test 6) reaches $p' = 0\text{kPa}$ in just 3 cycles, whereas the specimen subject to a CSR = 0.10 (Test 5) takes 65 cycles to reach $p' = 0\text{kPa}$.

When this state ($p' = 0\text{kPa}$) is obtained, the specimen has cyclically liquefied. This is different from flow liquefaction in monotonic tests as the specimen can still resist load – the stress path only passes through a state where $q = 0\text{kPa}$ and $p' = 0\text{kPa}$. This is best shown in Test 6 (CSR = 0.20). The stress path reaches $q = 0\text{kPa}$ and $p' = 0\text{kPa}$, but then begins to show an increase in compressive strength up to $q = 10\text{kPa}$ (the testing apparatus prevents this from increasing all the way to the target single amplitude stress of 40kPa). This ability to continue resisting load is accompanied by much larger strains than during the cycles away from $p' = 0\text{kPa}$, meaning the specimen has stiffness degradation. This is also shown in Figure 31(right-hand side).

These stress-strain plots show the relatively small axial strains experienced by the specimens during the early stress cycles (less than 1% axial strain). Then as the stress path moves closer to $p' = 0\text{kPa}$, the stiffness of the soil reduces and the strain increases. Also note that the larger the applied CSR, the further the specimen is strained. It is this issue (increasing soil displacement) that becomes a problem in the field. Sand deposits may still be able to resist load during an event such as an earthquake, but if cyclic liquefaction occurs the larger deformations can cause severe damage to infrastructure. This undrained cyclic testing can however be used to assess the likelihood of cyclic liquefaction being reached, through use of liquefaction curves.

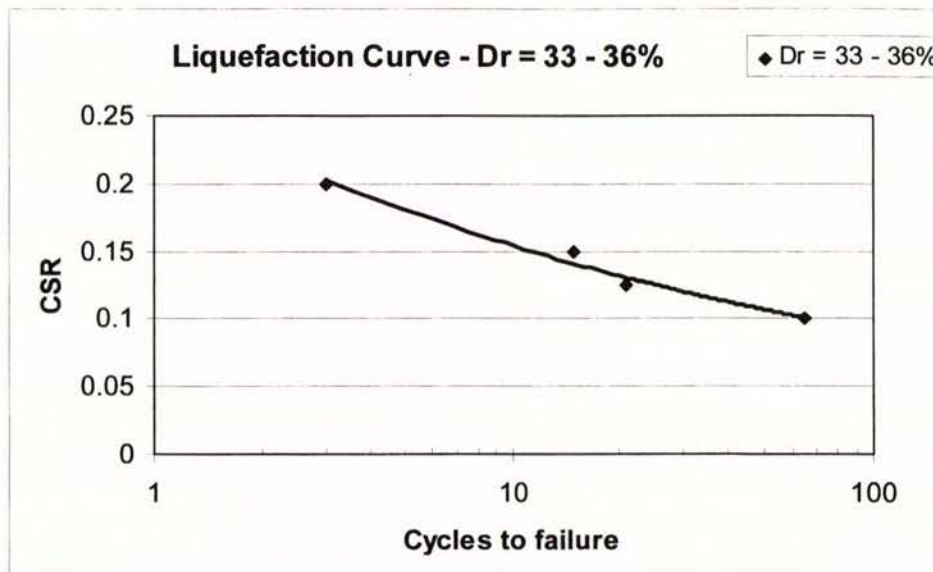


Figure 32 – Liquefaction curve derived from the undrained cyclic tests.

The liquefaction curve in Figure 32 is created by plotting the CSR of each test against the number of cycles to reach $p' = 0\text{kPa}$. Cyclic liquefaction is also considered as having occurred when the double amplitude strain reaches 5%. As shown above, these points create an approximately straight line when plotting the cycles on a logarithmic scale. Earthquake information can then be simplified into an estimate (for a given event) of CSR and total cycles. If this point plots to the right of the curve, cyclic liquefaction is likely to occur. If it plots to the left of the curve, the soil will most likely retain its stiffness. It is important to note however that this curve is only applicable to this sand (Albany Sand), at this tested density ($Dr = 33 - 36\%$), and prepared using the moist tamping placement method. The fabric of a soil plays a large part in undrained behaviour, and the curve would change if a dry pluviation placement method (for example) was used, even if specimen densities were kept the same.

5.4 Albany Sand Triaxial Testing Summary

Albany Sand was tested using the newly acquired triaxial testing apparatus. 13 test specimens were created and tested – these were completed using drained monotonic,

undrained monotonic and undrained cyclic loading conditions. This testing phase produced two major findings. The calibration of the triaxial apparatus was verified as being correct and suitable for use in future stages of the research. This was concluded as the test results showed behaviour expected of Albany Sand (in a qualitative sense). The testing also allowed the methods for apparatus use to be learnt, and the test procedures to be refined. This was done to in an attempt to obtain the best possible results from the next stage of testing, using local Christchurch sandy soil.

6. Triaxial Tests on Foundation Soils of Fitzgerald Bridge

The first major part of the PhD research is to investigate the effect of fine particles in sand on liquefaction. It was proposed that silty sand be taken from the Christchurch area and used as a triaxial test material. This involves using the sand-sized particles from the soil as a base material, and varying the fines (silt) content over the course of the testing. The aim is to compare the undrained behaviour of the sand at different fines content, enabling the creation of a model for predicting undrained behaviour for other silty sands in the field. Currently 30 triaxial tests have been completed on a locally sourced soil with 10% silt content by weight. This includes 13 undrained monotonic tests and 17 undrained cyclic tests. The results have shown typical silty sand behaviour, with a steady state line derived from the monotonic testing, and liquefaction curves obtained from the cyclic testing.

6.1 Fitzgerald Bridge Soil Mix

The traffic bridge crossing the Avon River on the corner of Fitzgerald Avenue and Kilmore Street in Christchurch is currently being upgraded. Part of this requires new piling, which has been investigated and designed by the geotechnical engineering firm Tonkin and Taylor. A site investigation was completed in June 2006, with a number of soil samples being taken along with SPT and CPT data. These samples were obtained for testing from Tonkin and Taylor after they no longer required them, in November 2006. Each soil sample was sieved to determine the soil PSD (Particle Size Distribution) up to the 75 μ m sieve. This size distinguishes between sand particle sizes and silt particle sizes.

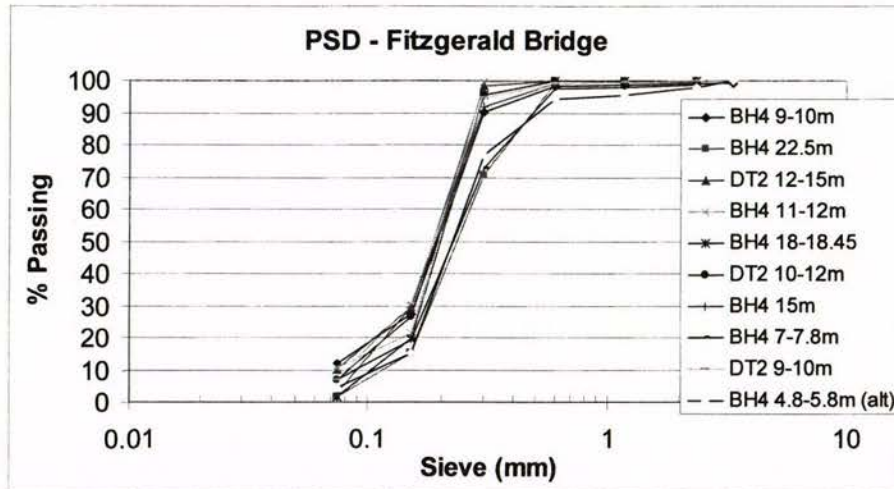


Figure 33 – Particle Size Distribution for soil samples taken from the Fitzgerald Bridge site.

It was determined from the distributions in Figure 33 that almost all samples were of silty sand containing fines in the range between 2 – 12%. A decision was made to mix together the samples with most similar distributions to create one homogeneous soil mix. This was completed by taking 7 samples and mixing small masses of each in a large container, until all 7 samples were combined sufficiently. This mixture is the Fitzgerald Soil Mix (FSM). This was also sieved to give a final PSD for the mix. As shown below in Figure 34, the FSM is a silty sand with a silt content of 10%.

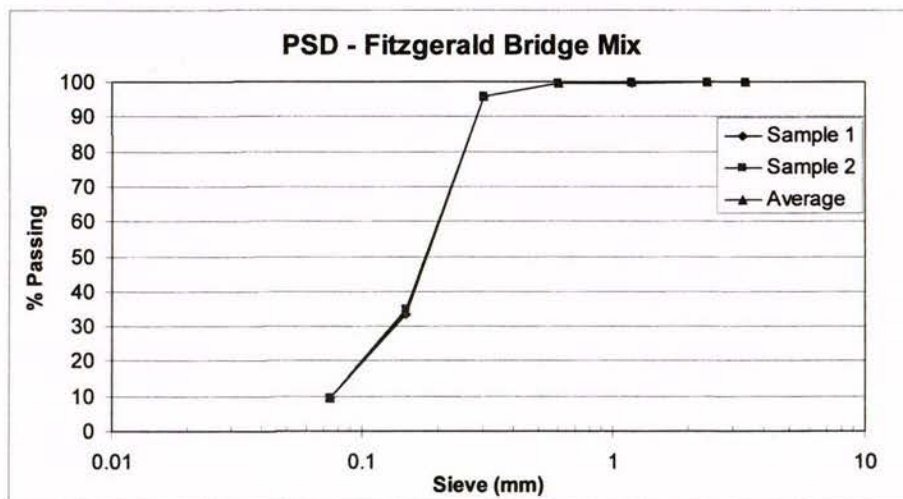


Figure 34 – Particle Size Distribution for the Fitzgerald Soil Mix.

This mixture was kept in a large sealable container throughout use in triaxial testing. The mixture was found to have a moisture content of 9 – 10%. A number of other materials such as small organic matter and fragmented shells were also noticed in the mixture during specimen preparation. This is due to the soil being taken directly from the field, at a river site.

The solid particle density (ρ_s) and maximum and minimum void ratios (e_{max} and e_{min}) were calculated using the British Standards BS 1377-2:1990 and BS 1377-4:1990 as loose guidelines. This gave the values shown in Table 5.

Table 5 – Fitzgerald Soil Mix properties.

Solid Particle Density - ρ_s	2.66 g/cm ³
Maximum Void Ratio - e_{max}	0.945
Minimum Void Ratio - e_{min}	0.597

6.2 Soil Preparation

The soil was prepared differently for the undrained monotonic tests and the undrained cyclic tests. The monotonic tests were completed first, and the sand was taken directly from the FSM container, lightly ground to separate the particles, and then placed in the specimen mould for moist tamping. This meant the soil was at a moisture content of 9 – 10%. After monotonic testing, the sand was carefully washed out of the specimen membrane and dried in an oven. This sand was retained by placing into another separate container.

Before cyclic testing begun, it was determined that not enough of the original FSM remained to complete the tests. The sand previously tested and dried during the monotonic stage was therefore selected to be used. This was lightly ground to separate the clumps of silt, weighed in batches, and de-aired water mixed in to bring the soil up to a moisture content of 9%. This was then ready to be placed for moist tamping.

6.3 Specimen Preparation

All specimens were created using the procedure described in Section 4. The only differences were the amount of sand and moist tamping required for each specimen density. All other steps were kept constant until specimen loading was begun.

6.4 Undrained Monotonic Triaxial Tests

A total of 13 specimens were prepared and tested using undrained monotonic loading. All specimens were isotropically consolidated. An initial effective confining pressure (p') of 100kPa was applied to the specimens, except for Test 12 where the initial $p' = 200$ kPa. All specimens were axially displaced at a rate of 0.3mm/min. Details of specimen densities are outlined in Table 6.

Table 6 – Test specimen properties for the undrained monotonic tests.

Test Number	Void Ratio – e_{test}	Relative Density - D_r	Skempton's B-value
1	0.821	36 %	0.97
2	0.838	31 %	0.95
3	0.854	26 %	0.97
4	0.863	24 %	0.98
5	0.828	34 %	0.98
6	0.847	28 %	0.97
7	0.806	40 %	0.99
8	0.814	38 %	0.97
9	0.780	47 %	0.97
10	0.744	58 %	0.95
11	0.725	63 %	0.95
12	0.829	33 %	0.99
13	0.691	73 %	0.99

Note that the void ratios (and relative densities) used in Table 6 were calculated using pre-test soil mass weights and specimen dimension measurements. This creates some

uncertainty in the density calculations, as the looser specimens tended to have visible ‘dents’ in their fabric which could not be accounted for in terms of volumetric significance. This led to the post-test density evaluation method being created mid-way through this testing phase. However, the densities are listed using the pre-test evaluation method in the interests of maintaining uniform data.

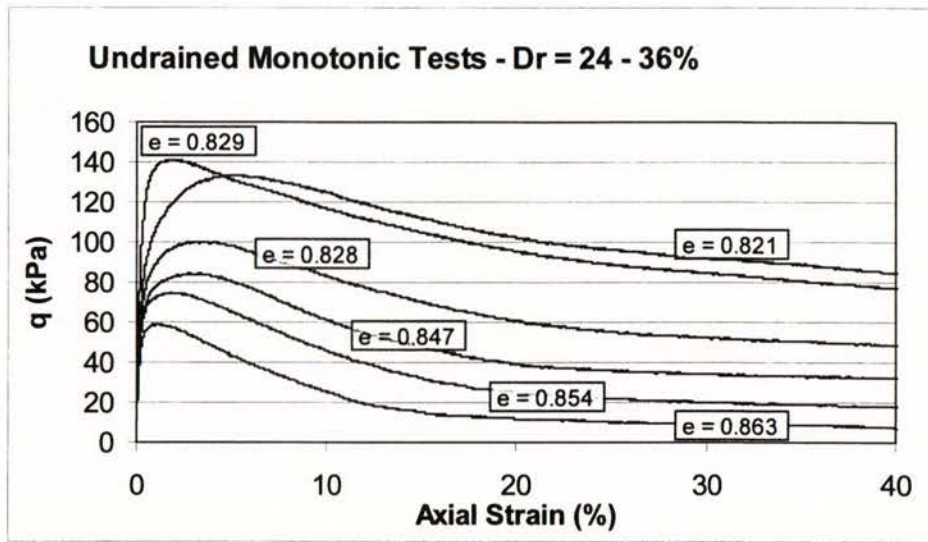


Figure 35 – Stress-strain behaviour of monotonic test specimens between $Dr = 24 - 36\%$. Specimens were tested at an initial effective confining pressure $p' = 100\text{kPa}$, except for $e = 0.829$ (initial effective confining pressure $p' = 200\text{kPa}$).

The behaviour of the looser specimens ($Dr = 24 - 36\%$) is very similar. Figure 35 shows each of the specimens reaching a peak deviator stress before around 5% axial strain, followed by a drop in strength (strain softening). Note that Test 12 ($e = 0.829$) reaches a peak strength much earlier than Test 1 ($e = 0.821$). This is due to the effect of the higher initial effective confining pressure $p' = 200\text{kPa}$. In general, the denser specimens appear to reach peak strength at higher strains than the looser specimens.

Steady state for these specimens is considered to occur at 30 - 40% axial strain, with Figure 35 showing the deviator stress (q) relatively constant at this strain level. As expected the steady state strength drops as the specimen density is reduced, with the loosest specimen ($e = 0.863$) almost achieving static liquefaction.

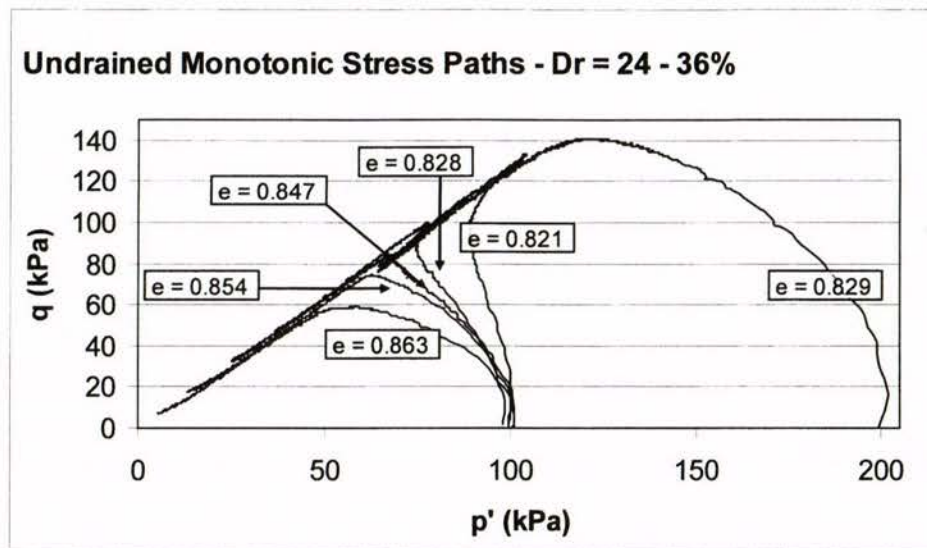


Figure 36 – Undrained monotonic stress paths for test specimens between $Dr = 24 - 36\%$.

The undrained stress paths in Figure 36 give further information on the behaviour of the specimens. The looser test specimens ($e = 0.863, 0.854, 0.847$) show highly contractive behaviour, as these specimens experience a decreasing p' throughout the loading. The slightly denser specimens tend to show some dilative behaviour (increasing p'), although all eventually experience contractive behaviour. The effective stress failure line can be estimated as $q/p' = 1.25$.

An interesting result is seen in Test 1 ($e = 0.821$). The stress path appears to move up the effective stress failure line, indicating that the specimen will continue with dilative tendencies. However, the specimen changes to contractive behaviour (at peak strength) and the path moves down towards the origin. Such a sharp direction change in the stress path may be due to significant non-uniformity and change in specimen shape at large deformations.

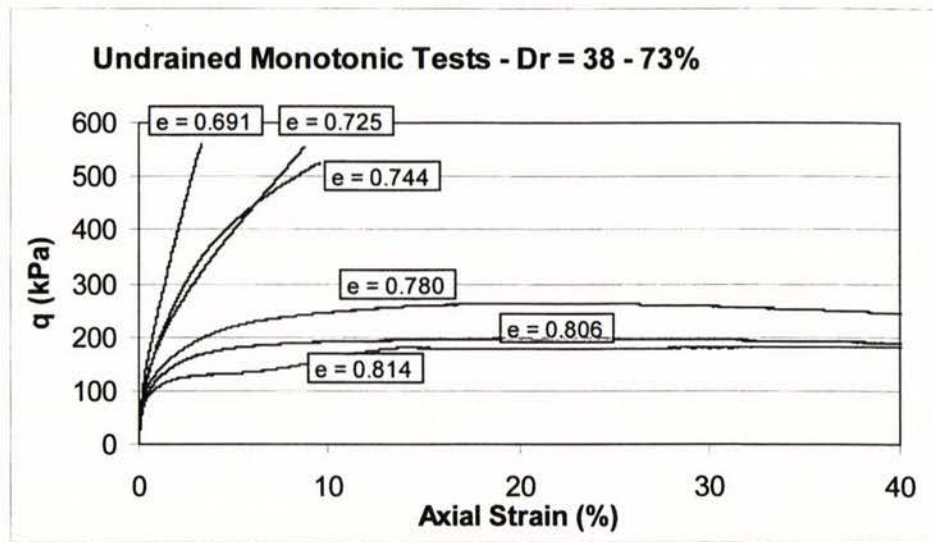


Figure 37 - Stress-strain behaviour of monotonic test specimens between $Dr = 38 - 73\%$.

The behaviour of the denser specimens ($Dr = 38 - 73\%$) is typical for a silty sand. Figure 37 shows an increasing deviator stress (q) with increasing axial strain, with no significant drop in strength occurring. This means that the specimens are not experiencing strain softening. Instead the specimens reach a peak strength, and retain that strength as the axial strain is increased to 40%. This means that the peak strength is also approximately the steady state strength. Note however that some tests were stopped before reaching 40% axial strain. This was due to specimens shifting over the edge of the end caps (due to increasing specimen diameter) during straining (shown in Figure 38), meaning that the applied axial stress on the specimens could no longer be accurately calculated. The pore pressure also dropped below 0kPa in these tests – the curves in Figure 37 have been stopped at this point, as the data becomes unreliable beyond this limit.

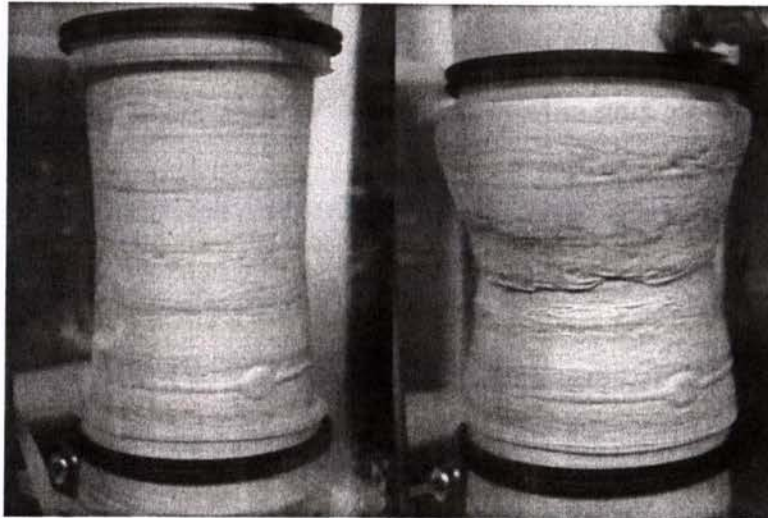


Figure 38 – Test 10 specimen ($e = 0.744$) at 10% axial strain (left) and 30% axial strain (right). Note that the specimen diameter exceeds the top cap diameter at 30% strain.

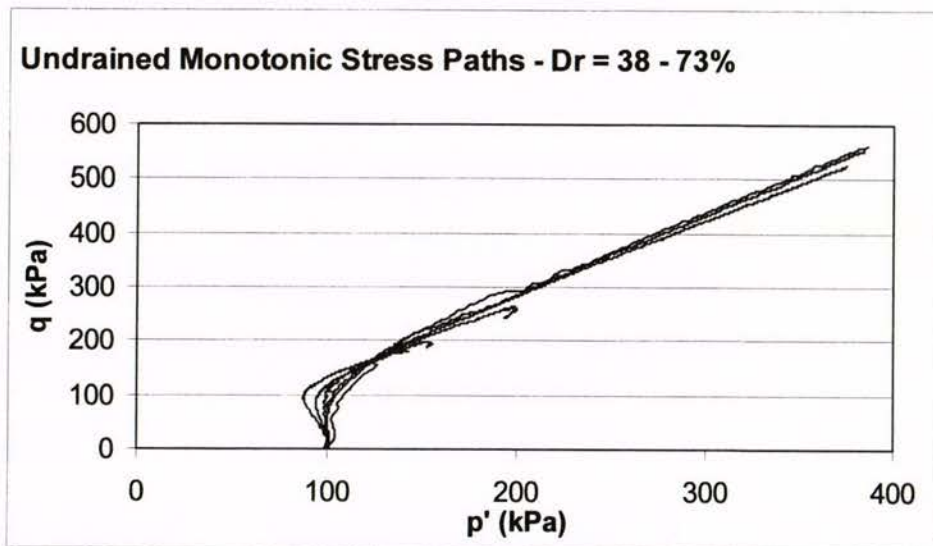


Figure 39 - Undrained monotonic stress paths for test specimens between $Dr = 38 - 73\%$.

Figure 39 shows the undrained stress paths for the denser specimens ($Dr = 38 - 73\%$). It shows the highly dilative nature of the specimens, as p' generally experiences only a small drop before increasing. Note that the effective stress failure line can be clearly made out in Figure 39 (the line the paths move up), and has a slope of approximately 1.4 when using this plot. The steady state values of p' for all specimens are taken from these undrained stress path plots and used to create a steady state line for the soil mixture.

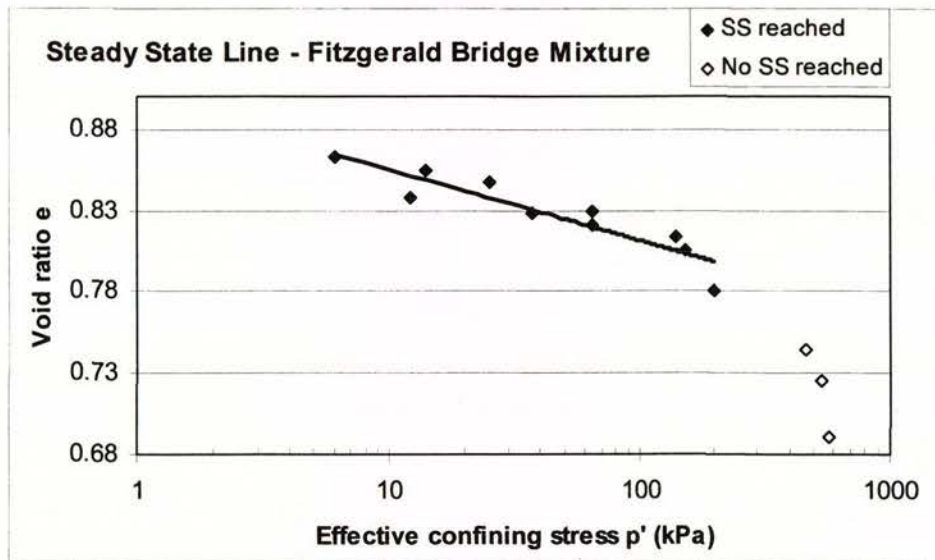


Figure 40 – Steady state line for the Fitzgerald Soil Mixture obtained from undrained monotonic testing.

The steady state line in Figure 40 is created from the steady state points obtained from specimens during undrained monotonic testing. The line is plotted with p' in log scale. Note that there is scatter in the data points – this is in part due to the issues with exactly identifying the specimen void ratio, and also the inherent variability of specimens created using natural sand for triaxial testing. The data points for the denser specimens are shown in Figure 40 as open symbols – this represents the fact that steady state was not reached in these tests. The actual steady state for these specimens would lie to the right of these points.

The steady state line does help to predict the behaviour of any specimen created using the Fitzgerald Soil Mix. Undrained loading causes no change in specimen density, and therefore specimen paths will move horizontally in the $e - p'$ plane. A specimen with initial conditions (void ratio, p') to the right of the steady state line will move left, showing contractive tendencies. The opposite applies for specimens with initial conditions to the left of the steady state line. Such specimens will have dilative tendencies, with strain softening unlikely to occur.

6.5 Undrained Cyclic Triaxial Tests

A total of 17 specimens were prepared and tested using undrained cyclic loading. All specimens were isotropically consolidated. An initial effective confining pressure (p') of 100kPa was applied to all specimens. All specimens were axially loaded with differing Cyclic Stress Ratios, using a sinusoidal loading pattern with a period of 2 minutes. Details of specimen densities are outlined below in Table 7.

Table 7 – Test specimen properties for the undrained cyclic tests.

Test Number	Void Ratio – e_{test}	Relative Density - D_r	Cyclic Stress Ratio (CSR)	Skempton's B- value
14	0.818	36 %	0.225	0.97
15	0.805	40 %	0.150	0.97
16	0.815	37 %	0.192	0.98
17	0.823	35 %	0.121	0.98
18	0.786	46 %	0.233	0.98
19	0.788	45 %	0.196	0.97
20	0.785	46 %	0.151	0.98
21	0.791	44 %	0.257	0.95
22	0.744	58 %	0.279	0.97
23	0.747	57 %	0.239	0.98
24	0.740	59 %	0.200	0.97
25	0.736	60 %	0.175	0.98
26	0.740	59 %	0.316	0.97
27	0.710	68 %	0.284	0.97
28	0.711	67 %	0.218	0.98
29	0.711	67 %	0.349	0.96
30	0.707	68 %	0.180	0.95

Note that the void ratios (and relative densities) used in Table 7 were calculated using post-test soil mass weights. This is due to the post-test values showing better consistency than the pre-test values.

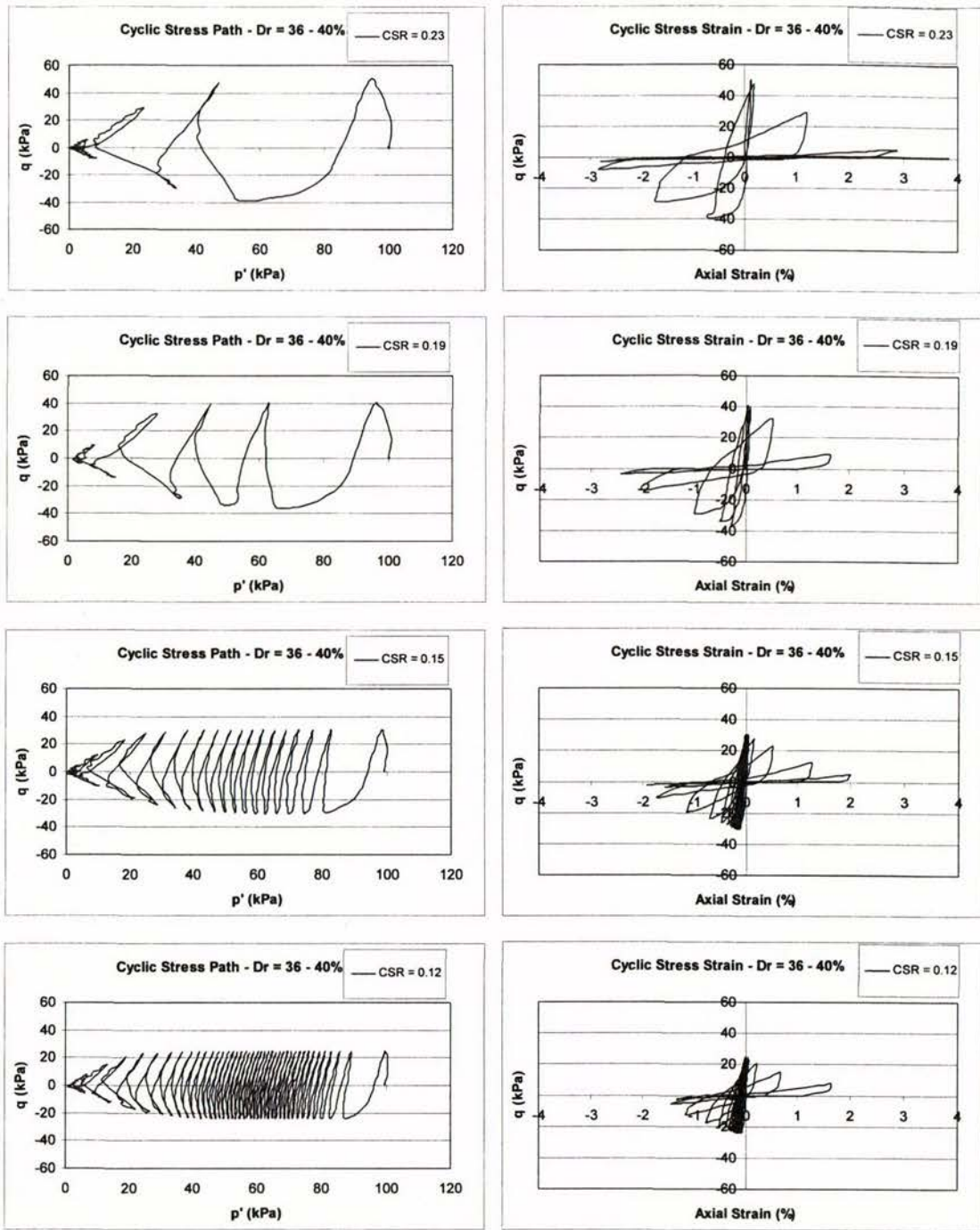


Figure 41 – Stress path and stress-strain behaviour of cyclic test specimens between $Dr = 36 - 40\%$.

Figure 41 shows typical stress-strain behaviour (right-hand side) for similar-density specimens tested under cyclic loading. The initial cycles of each test are completed with

experienced during the initial cycles. However, as strain softening begins to take place the extension strains (negative axial strains) increase beyond the value of the compression strains. This is consistent with sandy soil behaviour, as it is more difficult for the soil fabric to resist extension loading due to sand grain alignments. It should also be noted that for similar CSR values, the denser specimens display lower axial strains at nearly zero p' than for the looser specimens. This is again expected, as denser specimens tend to resist higher loads and deformations.

The undrained cyclic stress paths for the looser specimens are shown in Figure 41 (left-hand side). All specimens reach $p' \approx 0\text{kPa}$, the point at which initial cyclic liquefaction occurs. The difference in each test is the CSR applied to the specimens and the response this causes. The main result of higher CSR application is the number of cycles it takes to reach cyclic liquefaction. As shown in Figure 41, the specimen tested at $\text{CSR} = 0.23$ only takes a few cycles to liquefy. The stress path rapidly moves towards the origin, with a drop in effective confining stress of around 60kPa in the first cycle. The specimen tested at $\text{CSR} = 0.12$ takes much longer (40 cycles) to reach cyclic liquefaction. As can be seen in Figure 41, the stress path in this test has smaller drops in p' between each cycle, and moves towards the origin more slowly than the $\text{CSR} = 0.23$ test.

Similar behaviour can be seen in Figure 42 (left-hand side) for the denser test specimens, as initial cyclic liquefaction occurs much faster (in less cycles) for the specimens tested at higher CSR. Another feature that can be more easily seen in Figure 42 is the effective stress failure envelope. This is the same line as described for the monotonic tests, except with another boundary on the extension loading side of the plot, creating an envelope. This is best displayed by the test with an applied $\text{CSR} = 0.35$. After passing through $p' = 0\text{kPa}$, the stress path follows the envelope and the specimen experiences and increasing q and p' .

It is difficult to compare the effects of density on cyclic liquefaction when using cyclic stress paths. Therefore cyclic liquefaction curves are created, plotting the applied specimen CSR with the number of cycles taken to reach initial cyclic liquefaction. This

testing will be used to develop a correlation between undrained monotonic and cyclic behaviour, as well as in assessing the effect of fines in sand liquefaction.

6.6 Fitzgerald Soil Mix Triaxial Testing Summary

The Fitzgerald Soil Mix was tested using the triaxial testing apparatus. 17 test specimens were created and tested – these were completed using undrained monotonic and undrained cyclic loading conditions. This testing phase produced two major findings. The steady state line for the soil mix was derived, enabling the undrained monotonic behaviour of the soil to be predicted before loading takes place. For example, it can be determined using initial specimen state conditions whether a specimen will show contractive or dilative tendencies during the application of axial strain. The second result was the liquefaction curves for the soil mix, taken from data obtained during cyclic loading tests. These curves identify the required cycles at a particular Cyclic Stress Ratio (CSR) for a specimen to reach initial cyclic liquefaction (zero effective confining stress). Four curves in total were defined, each for a different specimen density.

It is estimated that this second test phase will take around two months to complete, as a maximum of 4 tests per week is possible.

7.2 Silty Sand Testing

A final third phase of testing will be completed using the Clean Fitzgerald Soil Mix as a base material. Fines will be added to this mixture to create a soil with between 30 – 40% fines by weight. These particles will most likely come from the Ferrymead Soil Sample taken in April 2006 from the Ferrymead area of Christchurch. Again this new soil mixture will be put through sieves to allow the PSD to be determined. The maximum and minimum void ratios will also be defined.

The triaxial testing of this soil mixture is planned to follow the same procedure as for the first and second phases of testing (moist tamping etc). However the higher silt content may require some aspects of the preparation to be slightly altered. This will not become clear until the actual test preparation begins. It is planned that some of the test specimens for this stage will have the same void ratios and relative densities as specimens in the first and second test stages, to again allow direct comparison using these parameters. This will be very useful when developing the silty sand characterisation model.

7.3 Silty Sand Characterisation Model

This model will be developed from the beginning of the second test stage through until after the third test stage is completed. It will involve assessing the behaviour of the monotonic and cyclic test specimens, with particular interest in the initial conditions of the specimens (relative density, void ratio, state parameter, state index, void ratio difference). The aim will be to define a parameter from the list above, or create a new one, that will help characterise many sands containing fines in terms of undrained behaviour. This parameter will then be used in a new model for predicting this behaviour

model predictions will also vary the time required for this stage, depending on how the results turn out. It may be that a small amount of samples are required to sufficiently assess the reliability of the model, or it may require a larger number of samples. It is currently thought that 5 – 8 samples from different sites should provide enough data for this assessment.

- Seed, H. B. (1987). "Design Problems in Soil Liquefaction." *Journal of Geotechnical Engineering*, 113(8), 827-845.
- Seed, H. B., and Idriss, I. M. (1982). *Ground Motions and Soil Liquefaction during Earthquakes*, Earthquake Engineering Research Institute, California.
- Seed, H. B., Tokimatsu, K., Harder, L. F., and Chung, R. M. (1985). "Influence of SPT Procedures in Soil Liquefaction Resistance Evaluations." *Journal of Geotechnical Engineering*, 111(12), 1425-1445.
- Verdugo, R. (1992). "Characterization of Sandy Soil Behaviour under Large Deformation," University of Tokyo, Tokyo.
- Yamamuro, J. A., and Covert, K. M. (2001). "Monotonic and cyclic liquefaction of very loose sands with high silt content." *Journal of Geotechnical and Geoenvironmental Engineering*, 127(4), 314-324.
- Youd, T. L., and Idriss, I. M. (2001). "Liquefaction resistance of soils: Summary report from the 1996 NCEER and 1998 NCEER/NSF workshops on evaluation of liquefaction resistance of soils." *Journal of Geotechnical and Geoenvironmental Engineering*, 127(4), 297-313.
- Zlatovic, S. (1994). "Residual Strength of Silty Soils," University of Tokyo, Tokyo.